BIOLOGICALLY INSPIRED LOCOMOTION CONTROL OF BIPEDAL ROBOT

FENG KAI

(B.Eng., Harbin Inst. of Tech.)

A THESIS SUBMITTED
FOR THE DEGREE OF MASTER OF ENGINEERING
DEPARTMENT OF MECHANICAL ENGINEERING
NATIONAL UNIVERSITY OF SINGAPORE

2006

Summary

Due to recent growing popularity of humanoid robots in academia and industry, the bipedal locomotion control has become a fundamental issue of legged robotics. In this thesis, we develop a simple control strategy based on biological inspiration to control the locomotion of a bipedal robot. The control strategy utilizes a set of coupled neural oscillators to mimic the neural activities of the Central Pattern Generator (CPG) that is found at the spinal cord of many vertebrate animals. The control strategy is tested on a ten Degrees of Freedom (DOF) model of bipedal robot. Simulation results suggest that due to the coupling of the neural oscillators of CPG and the feedback from the environment, the algorithm can generate stable and coordinated walking patterns of the bipedal robot on both level and uneven ground.

Keywords: bipedal robot, locomotion, central pattern generator, neural oscillator, motor control

Acknowledgement

I would like to take the chance here to express my sincere thanks to many people who make the completion of the thesis possible.

First of all, I would like express my thanks to my supervisors, Dr. Chew Chee Meng and Prof. Hong Geok Soon, for leading me to the fascinating world of humanoid robotics and their patience and timely guidance through out my whole period of study.

I would like thank all the colleagues in the Legged Locomotion Group , H. H. Nghia, T. Sateesh, W.Y. Sim and W. Zhou. Without many inspirational discussions with them, the writing of this thesis would be much more difficult.

Thanks should also goes to the technical staffs in Control & Mechatronics Lab, Ms. Tshin, Ms. Ooi, Ms. Hamilda and Mr. Zhang for their logistic and technical help.

Special thanks to my parents, for their continuous encouragement.

Table of contents

List of Tables

List of Figures

Chapter 1

Introduction

1.1 Background

Bipedal robots have been drawing much attention during recent years. The boom of bipedal robots can be traced back to 1970s when the late Professor Ichiro Kato and his robotics group at Waseda University initiated the Cabot project. Cabot-1 was the first life-size robot which demonstrated basic bipedal walking capability. Since then numerous bipedal robots are being introduced by universities and research institutes as well as companies like Honda [Hirai et al. (1998)] and Sony [Nagasaka et al. (2004)], for either research or entertainment purposes.

However, despite the increasing number of bipedal robotics platforms, locomotion control has not gained much significant advancement. To make bipedal robots walk stably and naturally is still a difficult engineering endeavor. Among those systems that have been developed only a small fraction can achieve dynamic walking with high speed [Plestan et al. (2003)].

The lack of locomotion capability has increasingly become a bottleneck for the de-

Figure 1.1: Humanoid robots by companies and research institutes: Upper left to right (life size) - Cabot-1 from Waseda University, Asimo from Honda Co., NUSBIP II from Legged Locomotion Group, NUS. Lower left to right (toy size) QRIO from Sony Co., VisiOn from Vstone Ltd., and ROPE IV from Legged Locomotion Group, NUS

velopment of bipedal robots. This is very much attributed to the complexity of bipedal mechanism for many reasons:

- Bipedal robots usually consist of many degrees of freedoms (DOF). A typical full

configuration bipedal robot has a total number of twelve joints.

- Bipedal robots are essentially multi-input multi-output (MIMO) nonlinear system with under-actuation. In addition, the dynamic of the robot is constantly changing and is unstable. It is thus hard for modeling and controller synthesization.

- Within a walking cycle when the robot make transitions from single support phase to double support phase, the interaction of the foot to the environment introduces additional dynamics to the system, which is also hard to analyze.

- The walking control is subject to many high level performance indices as well.

The performance indices here are not as well-defined as conventional robotics systems. And not meeting these indices may cause the whole control system to fail. One of the basic performance indices for a bipedal robot is movement coordination and posture stability. Other indices usually includes smoothness of motion, energy efficiency, adaptability to different ground condition and perturbation, actuator bandwidth and capacity requirement, etc.

1.2 Motivation of Bipedal Locomotion Research

The advantage of legged robots over other kinds of robots is obvious. The legged locomotion capability enables the robots greater versatility to maneuver complex and unstructured environments. A step of stairs could be easily cleared by legged robots, but it can be very hard for a wheeled robot to overcome.

The bipedal locomotion is the most advanced form of legged locomotion. It is found that animals with two legs show higher efficiency and better adaptability over multi-

legged animals [Vaughan (2003)]. A bipedal robot need also fewer linkage structures and actuators than a quadrupedal or hexapedal robot in order to walk.

Secondly, human being is bipedal. There are still many unanswered questions how human walking is organized. The research into bipedal locomotion control for robots helps us enhance our understanding of human walking in return.

And finally, giving consideration to the difficulties of developing a locomotion control strategy, bipedal robot is a perfect testbed for advanced control technologies and novel actuators.

1.3 Objective and Scope

Most locomotion control strategies so far are based on conventional control techniques. These strategies are often model based. And because of the high non-linearity and dynamic characteristics, these control strategies often fail to realize a sustained stable bipedal locomotion or the walking speed is too slow [Chevallereau et al. (2003)].

In this thesis, however, a different approach is taken as opposed to the model based control strategy. We utilize the biomechanical and the neurological inspirations in biological creatures as a general principle. The control strategy reproduces the neural activities from biological central nerve system called Central Pattern Generator (CPG).

The understanding of animal and human locomotion has provided us abundant resources to tap on when we design and control a bipedal robot. This approach is gaining growing popularity among robotics researchers. And it has been proven that this approach works decently well in decoupling a complex system which is hard to model [Dietz (2003)].

1.4 Contributions

The main contributions of the thesis are:

- Introduction of the bipedal locomotion and Central Pattern Generator (CPG) from a biological perspective.
- Performance analysis of two widely accepted mathematical model of neural oscillator (NO). Development of a simple bipedal locomotion control algorithm utilizing CPG that consists of four NO.
- Simulation and performance analysis of the control algorithm for a bipedal robot in simulation environment. Demonstration of the robustness of the algorithm under different environments and perturbation.

1.5 Thesis Organization

This thesis is organized into six chapters:

Chapter one introduces the scope and background of the bipedal locomotion research.

Chapter two gives a literature review on bipedal locomotion control. Several issues on walking control are addressed and two control strategies are presented.

Chapter three discusses the motor control systems in biological world. The concept of Central Pattern Generator is presented.

Chapter four presents two mathematical neuron models: Matsuoka neural oscillator (NO) and Van del Pol oscillator, which are commonly adopted by researchers for locomotion control. The basic properties of these two models are discussed.

Chapter five presents a control strategy that is based on CPG. The Matsuoka NO described in Chapter four is utilized to construct the CPG. A posture stability controller for ankle joints is also proposed in this chapter. Simulation results suggest the CPG model can generate a robust and adaptable walking pattern for the bipedal robot under different environment conditions.

Chapter six concludes the thesis and suggests future work.

Chapter 2

Bipedal Walking Control

The past few decades have witnessed a growing popularity of legged robots, especially bipedal robots that resemble human being. However the locomotion capability of the bipedal robots still remains as one of the essential technical challenges.

In this chapter we give a general review of research activities on bipedal walking control.

2.1 Literature Review

A mainstream approach of bipedal walking is to decentralize the control of the bipedal robot system into joint space and control each joint according to a prescribed reference trajectory [Huang et al. (2001)]. Some researchers specify the precalculated trajectory by observing human walking. However, since a bipedal robot has a very different mass distribution and much fewer actuating degree of freedom (DOF) compared to its human counterpart, the trajectory often needs to be modified significantly before it can be applied to the robot.

Another widely used approach is to apply sophisticated mathematical analysis of the robot kinematics and dynamics [Westervelt et al. (2003)]. The concept of ZMP (Zero Moment Point) introduced by Vukobratovic et al. (1989) is often utilized to analyze the stability of the trajectory. But as a bipedal robot is a highly nonlinear dynamic system, the analytical approach can only be applied to bipedal models with significant simplification. Moreover, since a bipedal robot is interacting with its environment all the time during its entire walking cycle, it makes the analysis even harder.

The difficulty of the trajectory-based approach has inspired some researchers to look into the basics of the animal and human walking. This resulted in many biologically inspired robots. Instead of prescribing a trajectory and letting the robot play it back, these approaches focus on the limit cycle behavior of legged locomotion. It is shown that limit-cycle-based motion control has a superior energy efficiency over the trajectory-based control [Fukuoka et al. (2003)]. The passive dynamic walker presented in McGeer (1990) is probably the first biologically inspired robot that utilizes the limit cycle behavior of the locomotion. By placing the passive walker on a slope, the bipedal walker converts its gravitational potential energy into kinematic energy to walk down the slope without any actuation in the joints. Recently several new passive dynamic walkers has been developed by MIT, Cornell and Delft University respectively [Collins et al. (2005)]. By introducing actuation, these dynamic walkers can walk on level ground. And the limit cycle behavior keeps the walking continuous.

Another group of biologically inspired robots are controlled by neural networks called Central Pattern Generator (CPG). The concept of CPG originated from the neurophysiological studies of vertebrate animals. Different forms of locomotion in animal life are characterized as rhythmic coordinated movement of limbs. However, the seemingly repetitive movement is under continuous subtle adaptations in a real-time manner which make it

possible for the locomotion movement to be sustained in the presence of environments changes such as a slope or a rough terrain. A CPG is a network of Neuron Oscillators coupled by mutual inhibition which can be used to control the limb movement of the robot and displays similar characteristics as life creatures. One example of legged robot controlled by CPG is Tekken [Fukuoka et al. (2003)], a quadruped robot developed in University of Electro-Communications in Japan. The CPG is applied to a four legged dog-like robot successfully and by changing some parameters in CPG, Tekken can fulfill different gaits such as rambling and trotting. No further dynamic analysis is required, and no trajectory is generated before hand and the robot is fully governed by the limit cycle behavior of the neural activities. So far although the CPG approach has not been implemented on any real bipedal robots yet, due mainly to actuator limitations, many simulations [Taga et al. (1991); Miyakoshi et al. (1998) and Jiang et al. (2000)] have been carried out and the results suggested that it can be a promising locomotion control methodology for bipedal robots in the future.

2.2 Static and Dynamic Walking

A bipedal walking can be classified as either static walking or dynamic walking. In static walking, the vertical projection of the Center of Gravity (CoG) of the robot always stays within the supporting area formed by the edge of feet that is in contact with the ground. In dynamic walking on the other hand, the CoG may leave the supporting area during the single support phase (Fig. 2.1).

Early researches in bipedal locomotion mainly focused in static walking because of its relative simplicity. However, one of the major drawbacks we can observe from static walking is that the robot has to shift its CoG from one leg to the other during every double

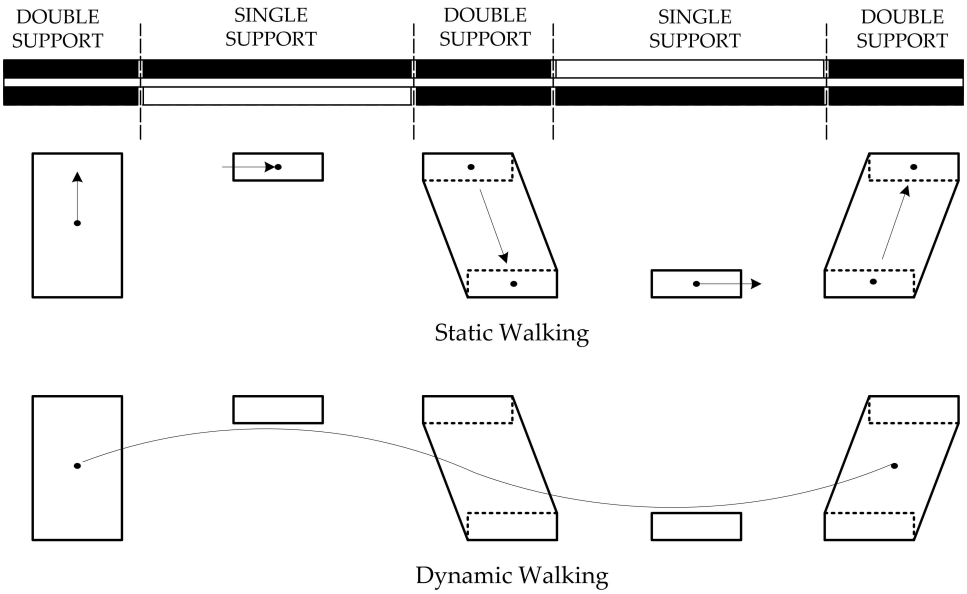

Figure 2.1: The CoG vertical projection during each support phase for static and dynamic walking. Position and trajectory of CoG are indicated by dot. The vertical projection of CoG trajectory is indicated by arrowed line (in static walking) and curve (in dynamic walking). Area of support during each phase is indicated by the solid line of the polygons.

support phase and maintain it during the whole single support cycle. It greatly limits the maximal walking speed achievable relative to dynamic walking. Furthermore, because a bipedal robotics system is typically constructed with rigid structure and heavy load of hardware especially actuators, the shift of CoG usually requires drastic body movements. This usually makes the static gait look awkward and inefficient.

2.3 Zero Moment Point (ZMP)

In dynamic walking, the CoG projection no longer falls inside the supporting area. The robot is statically unstable, but it may still maintain the dynamic equilibrium. A good

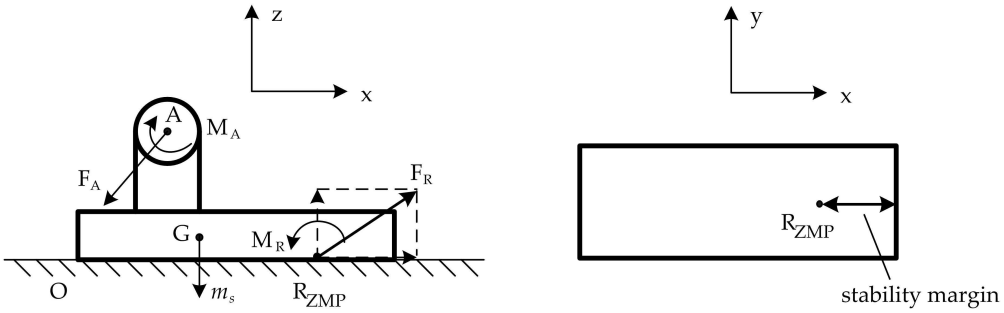

Figure 2.2: ZMP

example of dynamic stable mechanism is a balanced inverted pendulum by finger tip, as the supporting area is merely the contact point, and the CoG projection is always outside the supporting area.

In order to analyze the dynamic stability of robots, Vukobratovic et al. (1989) introduced the concept of ZMP (see Fig.2.2). Over the years different researchers use ZMP by slightly different interpretations [Li et al. (1991); Mitobe et al. (2000) and Okumura et al. (2003)]. But a well accepted definition of ZMP is given by Takanishi et al. (1985) as the point on the ground whereby the total forces and moments generated by gravity, inertia equals to zero:

$$F_A + F_R + m_s g = 0 \tag{2.1}$$

$$\overrightarrow{OA} \times F_A + M_A^o + \overrightarrow{OR} \times F_R + + M_R^o + \overrightarrow{OG} \times m_s g = 0 \tag{2.2}$$

where $\overrightarrow{OA}$, $\overrightarrow{OR}$ and $\overrightarrow{OG}$ are radius vectors from the coordinate origin to the ankle joint A, ZMP point R and foot mass centre G respectively. m_s is the foot mass. M_A^o and M_R^o are angular moment at ankle and ZMP w.r.t the origin.

If we take the ZMP as the origin of the coordinate, Eq.2.2 can be written as:

$$\overrightarrow{AR} \times F_A + M_A^R + M_R^R + \overrightarrow{GR} \times m_s g = 0 \tag{2.3}$$

From the above equations we can see that, the bigger M_A and the component of F_A along the $\overrightarrow{OX}$ is, the bigger the distance of ZMP w.r.t. the origin will be. In the extreme cases that the ZMP goes out the boundary of the foot area, the robot will tip over. This because of the unidirectional property of the moment M_R. If R is outside the supporting area of the foot, M_R could only be one direction (in the case shown in Fig.2.2, it is clockwise because the reaction force can only exists on the side of the foot which is resting on the ground). Since all other terms in Eq.2.2 are in clockwise direction as well, Eq. 2.2 will never be satisfied.

Thus the sufficient condition for the robot dynamic equilibrium is that the ZMP of the robot always stays in the supporting area of the robot. The longer the distance of ZMP w.r.t. the foot boundary is, the greater the stability margin of the robot.

In practice the force F_A and moment M_A at the ankle joint A are difficult to measure directly. However, it can be derived indirectly by measuring the dynamics of all the upper links of robot, and this gives the ZMP position in following equations:

$$x_{zmp} = \frac{\sum_{i=1}^{n} m_i(\ddot{z}_i + g)x_i - \sum_{i=1}^{n} m_i \ddot{x}_i z_i - \sum_{i=1}^{n} I_{iy}\ddot{\Omega}_{iy}}{\sum_{i=1}^{n} m_i(\ddot{z}_i + g)} \tag{2.4}$$

$$y_{zmp} = \frac{\sum_{i=1}^{n} m_i(\ddot{z}_i + g)y_i - \sum_{i=1}^{n} m_i \ddot{y}_i z_i - \sum_{i=1}^{n} I_{ix}\ddot{\Omega}_{ix}}{\sum_{i=1}^{n} m_i(\ddot{z}_i + g)} \tag{2.5}$$

where m_i is the mass of ith link, I_{ix}, I_{iy} and $\ddot{\Omega}_{ix}$, $\ddot{\Omega}_{iy}$ are the inertia and angular acceleration of ith link w.r.t. x-axis and y-axis [Huang et al. (2001)].

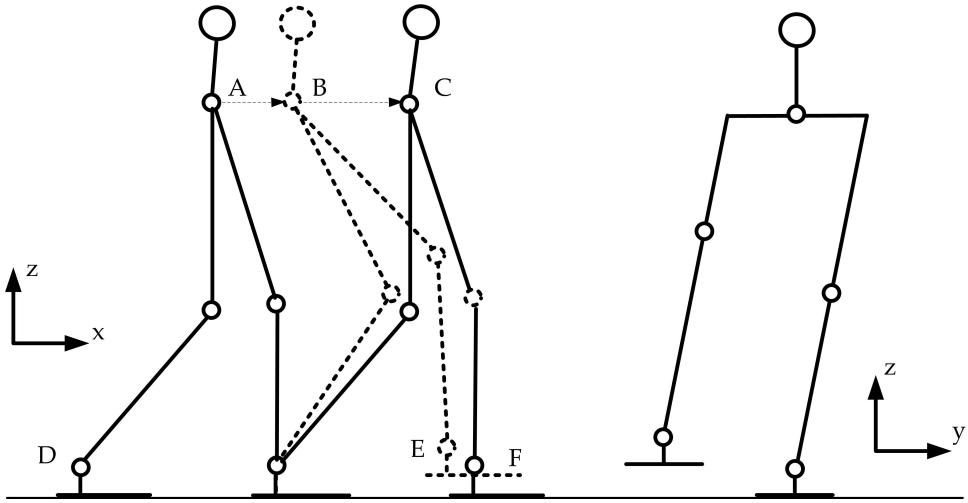

Figure 2.3: Multi-link Model of bipedal robot. Left: Sagittal Plane. Right: Frontal Plane.

2.4 Inverse Kinematics

The most widely used control strategy for bipedal locomotion is based on inverse kinematics. Consider a bipedal robot shown in Fig. 2.3. Given the coordinates of the hip with respect to the stance leg, the individual joint angles at both legs can be explicitly obtained. The control of the walking pattern is translated from the Cartesian space to joint space. In Fig. 2.3, A, B and C are predefined interpolation points of hip and D E and F of ankle joint of the stance leg of a half walking cycle. Once these points are specified, the trajectories for all joints of the stance leg can be easily calculated by the $A - B - C$ trajectory and trajectories for all joints of the swing leg can be calculated by the $D - E - F$ trajectory using inverse kinematics.

Inverse kinematics are being adopted by researchers mainly because it is a quick and straightforward way to generate walking pattern. However the walking speed is much limited by the model as it doesn't take dynamics into consideration. Most walking patterns generated by inverse kinematics are static walking.

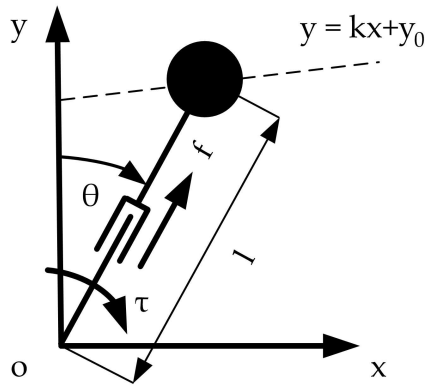

Figure 2.4: Linear Inverted Pendulum Mode

2.5 Linear Inverted Pendulum

Kajita and Tani (1996) proposed a model of bipedal walking called Linear Inverted Pendulum Mode(LIPM).

In LIPM, the walking cycle of the robot in sagittal plane is partitioned into two single support phase of alternative stance legs, with an instantaneous double support phase in between, during which the stance leg alternates. The bipedal robot during a single support phase can be treated roughly as an inverted pendulum consisting of a mass with a massless leg (stance leg).

The link length of the robot is variable such that the mass trajectory follows a constraint slope:

$$y = kx + y_o \tag{2.6}$$

By imposing such a constraint, the dynamics of the robot can be expressed in the following motion equations:

$$km\ddot{x} = f\cos\theta - mg \tag{2.7}$$

$$m\ddot{x} = f \sin\theta \tag{2.8}$$

where f is the translation force along the stance leg. Remove f by combining Eq. 2.7 with 2.8, the model can then be expressed in a simple linear differential equation:

$$\ddot{x} = \frac{g}{y_c} x \tag{2.9}$$

Solving the above equation gives the trajectory of the robot:

$$x(t) = x(0)\cosh(\frac{t}{T_c}) + T_c\dot{x}(0)\sinh(\frac{t}{T_c}) \tag{2.10}$$

$$\dot{x}(t) = \frac{x(0)}{T_c}\sinh(\frac{t}{T_c}) + \dot{x}(0)\cosh(\frac{t}{T_c}) \tag{2.11}$$

The double support phase in LIPM is instantaneous. A full walking cycle is completed by two consecutive single support phase of different stance legs. The foot placement of the swing leg can be calculated by simple geometry such that the transition doesn't result in serious kinetic energy loss.

Based on the LIPM, the thigh-shank mechanism of the stance leg of the bipedal robot can be treated as the pendulum with variable length. The knee joint is feedback controlled to limit the hip joint to follow the constraint line. The hip joint is controlled to keep the body upright. Fig.2.5 shows the tracking of the LIPM trajectory.

Ideally, given an initial velocity of the body, the mass will follow the prescribed trajectory even without controlled torque at the ankle joint because of the imposed constraint. However in real case this is not possible because of two main reasons. First, the model is not perfect in capturing the full dynamics of the robot. Treating the body of the robot as

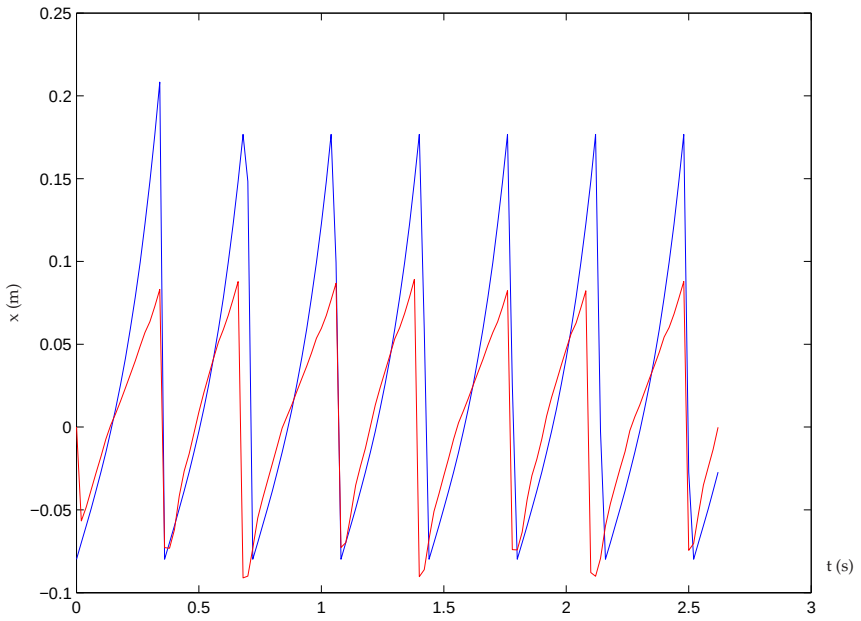

Figure 2.5: Trajectory tracking of LIP

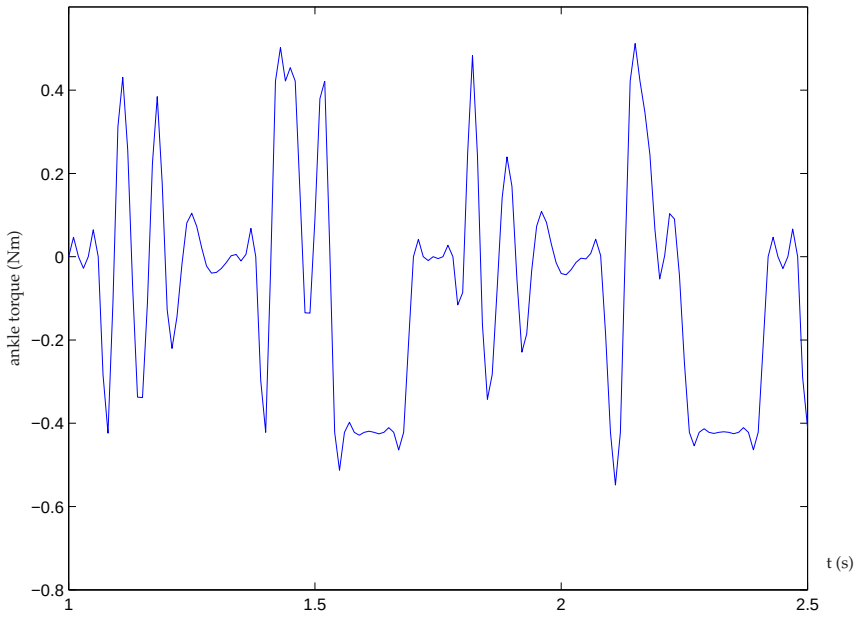

Figure 2.6: Torque at ankle joint

a point mass and the assumption of massless leg can lead to this imperfection. The other reason is that during each transition of stance leg, the impact of the foot with the ground will inevitably result in certain amount of kinetic energy loss. Thus the ankle joint must be controlled to track the prescribed trajectory in order to sustain the continuous walking pattern (see Fig. 2.6).

Chapter 3

Biological Locomotion

The common feature that various forms of locomotion in different animals shares is rhythmicity. How these walking patterns are generated and coordinated have been studied by researches from various disciplines such as neurophysiology, biomechanics and anatomy.

This chapter gives a brief explanation of walking from the biological perspective. The concept of CPG is introduced as a central motor control system for the locomotion.

3.1 Musculoskeletal System

Biological locomotion activities are carried out by musculoskeletal system. It consists of two separate yet interrelated sub-systems: muscular system and exoskeletal system. The musculoskeletal system functions as a basic kinetic and kinematic structure as well as source of actuation.

The exoskeleton system is a set of rigid bones that forms the basic shape of the animal. It provides physical support to the locomotor. Muscular system consists of skeletal muscles that are attached to the exoskeletal system by tendons across joints. The contraction of

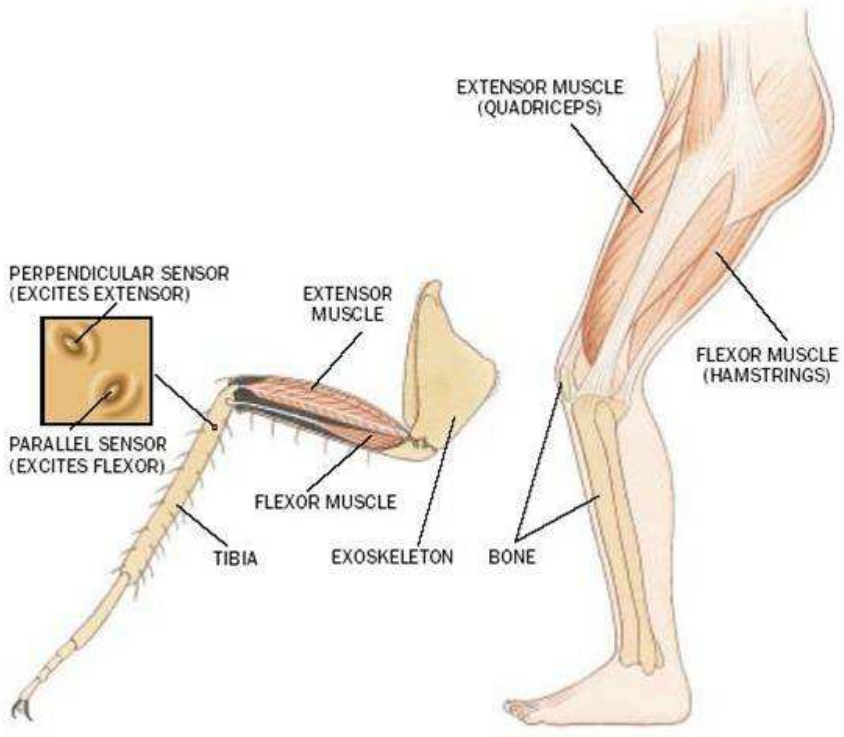

Figure 3.1: Musculoskeletal System. Reprint from Sasha and Seyfarth (1996)

muscles drives the bones around the joint. Generally speaking, skeletal muscles are organized in pairs of opposite direction such that as one group of muscles contracts, the other group stretches. These paired muscles are referred to as ”flexor” and ”extensor” muscles depending on their functionality. At any given time, only one muscle is stimulated. This property of muscle is called ”antagonism” [Kandel et al. (2000)].

Fig.3.1 shows the musculoskeletal system of insect and human being.

3.2 CPG as Motor Control System

The locomotion of animals can be characterized as a complex sequence of coordinated and rhythmic contractions of skeletal muscles [Winter (1990)]. The sequence of the rhythmic

muscular activities of flexor and extensor contraction constitutes a continuous walking pattern.

Early neurophysiology studies hypothesized that these motor patterns are produced by a complex network of neurons at the spinal cord. In Brown (1911) it is shown that cats with a partially transected spinal cord will lose its basic walking capability. However, it can still produce some rhythmic alternating contractions in ankle flexor and extensor. The hypothesis is further proven as cats decerebrated at lower brain level are able to step on a treadmill with an intact spinal cord. Thus it can be reasonably inferred that the rhythmic motor pattern are generated at the spinal cord level.

After Brown's seminal work, experiments conducted by many other researchers have shown evidences that such neural network that produces the rhythmic output not only exists in cats but also in many other vertebrate animals (for a detailed review, see Dietz (2003)).

These neural networks in spinal cord that generate rhythmic motor pattern are generally referred to as Central Pattern Generator (CPG).

3.3 Properties of Biological CPG

3.3.1 Structure of Motor Neuron

CPG consists of vast number of neurons. Fig.3.2 shows a typical structure of motor neuron at spinal cord. The neurons are interconnected by synapses. Cell body is also known as Soma and is the main body of the neuron. Dendrites are trunks of numerous cellular extensions, which receive nerve signals from other neurons. Axon is the output channel of a neuron. Axon branches off further to a number of axon terminals, where synapses to

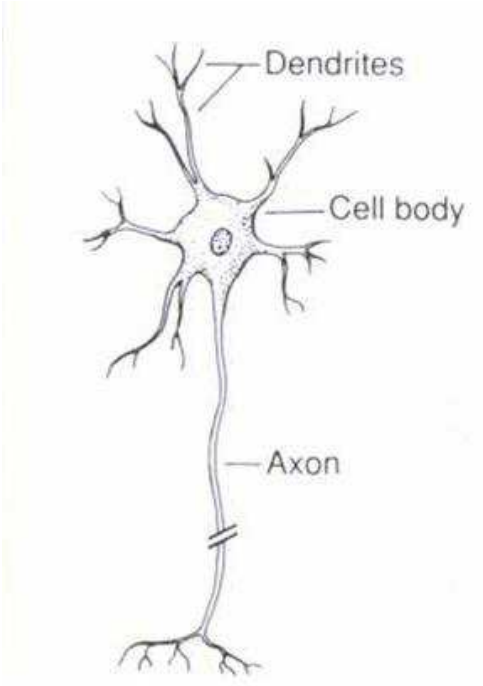

Figure 3.2: Structure of a Typical Motor Neuron. Reprint from Kandel et al. (2000)

other neurons are connected.

3.3.2 Stretch-Reflex

The stretch reflex is most fundamental property of muscles. Consider a pair of flexor and extensor muscles. When the flexor is contracted, the extensor is stretched because of the skeletal structure. This stretch will give rise to an even faster contraction of the extensor afterwards, in effort to regain its original length. Neuro-physiological studies suggest this stretch reflex behavior is due to the interactive effect of the flexor and extensor neurons [McMahon (1982)]. The monosynaptic connections between the two neurons makes them inhibit each other. Since the flexor and extensor are connected to the same joint and act in opposite directions, if both neurons are properly stimulated, an rhythmic oscillation at

the joint will emerge from the intermittent contractions of the two neurons.

The coupling of the counteractive neurons forms the basic unit of CPG. Because of the oscillatory pattern it displays, the mutually inhibitive flexor/extensor neuron pair is called a Neural Oscillator [Feng et al. (2005)].

3.3.3 Inter-neuron Connection

During the walking cycle of animals, a large number of muscles are involved. Since the muscles are controlled by individual neurons of CPG, and neurons are hardly intelligent, various properties of walking patterns such as coordinate and fixed phase lag must be the result of the organization of CPG. This is realized in inter-neuron connections.

The way the CPG network is structured and the weight of synaptic connections between neurons in nature have been evolving and perfecting over the ages.

3.3.4 Afferent Feedback to CPG

Despite that complete rhythmic motor patterns can be generated by isolated CPG, the actual motor pattern is constantly under regulation of afferent feedback [Grillner (1985)]. This feedback is established through monosynaptic connections from sensory neurons to motor neurons of the CPG. The internal motor program of CPG is then updated with information of the mechanical state of the limbs during their movement, thus making the locomotion activity a closed-loop system. The afferent feedback ensures the same motor pattern to be adaptable to different environment.

3.4 Summary

The increasing understanding of biological CPG has been inspiring robotics researchers to reproduce this biological motor control system in bipedal robot. However, the biological CPG is very complex, often exceeding the minimum requirement to generate the output motor pattern [Pearson (1993)]. Plus there are still many unanswered issues how exactly CPG works, especially in human. It is thus neither practical nor necessary to have a complete CPG model.

In the next chapter, two prevalent CPG models are introduced. The properties of the models will be discussed and compared with biological CPG.

Chapter 4

Modeling of CPG

The previous chapter discusses the basic principle that governs animal locomotion from a biological perspective. The periodical and rhythmic activities in locomotion of animals are generated by the Central Pattern Generator (CPG) at the spinal level. The concept of CPG and its relevance to locomotion is introduced. The CPG is a network of Neural Oscillators of mutually inhibiting neurons. To reproduce these oscillatory activities, a lot of researchers have been actively searching for proper mathematical models of the neural activities of CPG found in animals.

An individual neural oscillator is a couple of neurons that controls the extension (extensor neuron) and flexion (flexor neuron) of respective muscle. The flexor neuron and extensor neuron take excitive and inhibitive stimulus from each other and from neurons in other NO within the CPG network, as well as sensory stimulus feedback from the dynamic system. Each neuron also has a self-adaptation feedback to prevent its output becoming unbounded over time. The interconnection of these neurons and the dynamic system results in a rhythmic and coordinated output of the NOs with fixed period and phase difference [Friesen and Stent (1977)].

In this chapter two mathematical neuron models are presented. They are the most commonly adopted models by researchers in composing CPG network for bipedal locomotion. ASIMO

4.1 Matsuoka Neural Oscillator

4.1.1 Single Neuron Model

The first continuous-variable model of a single neuron was introduced by Morishita and Yajima (1972), as is shown below in Eq. 4.1-4.2:

$$\tau \dot{x} = -x + \sum_j w_j s_j \tag{4.1}$$

$$y = \max(0, x - \theta) \tag{4.2}$$

where x is the membrane potential of the neuron, s_j is jth input stimuli to the neuron and w_j is the synaptic connection weight of jth input, τ is the time constant, θ is the threshold value under which the the neuron doesn't fire, and y is the firing rate or output of the neuron.

The model had been widely used because of its mathematical simplicity. However, this model fails to deliver an essential characteristic of neuron in the real biological world. For real neurons, after receiving a step input stimuli, its firing rate will normally increase rapidly at first and then decrease gradually until it stabilizes at a lower level. This high-pass filter effect of neuron is called self-adaptation as was introduced by Luciano et al. (1978) and it plays an important role in the oscillatory activities. However, for the model shown in Eq. (3.1)-(3.2), the firing rate of neuron doesn't display such an adaptation, but

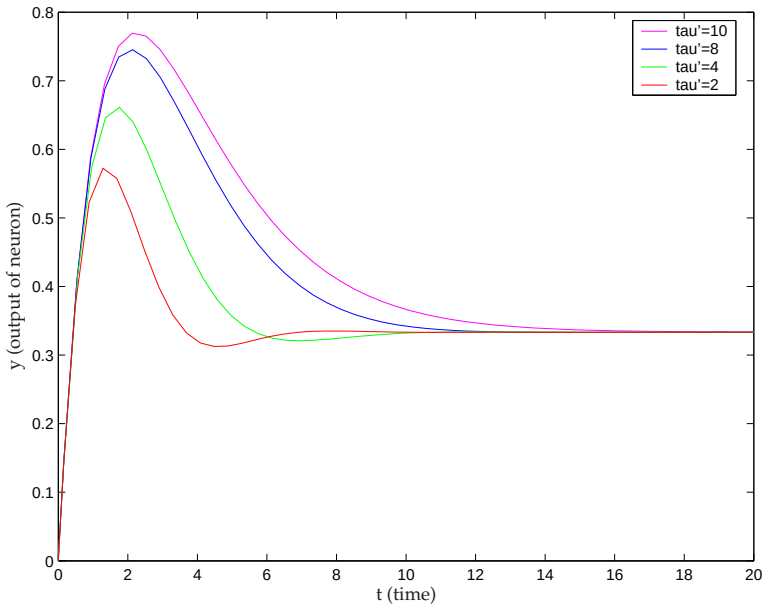

Figure 4.1: Step response of a single neuron with different value of self-adaptation rate. for all curves, $\tau = 1$, $\beta = 2$ and $\theta = 0$

rather increases monotonically until $x = \sum w_j s_j$.

Because of the limitation of the Morishita's model, Matsuoka (1985) propose a modified neuron model, which takes the self-adaptation into account. The model is shown below in Eq. (4.3)-(4.5):

$$\tau \dot{x} = -x + \sum_{j=1}^{n} w_j s_j - \beta v \tag{4.3}$$

$$\tau' \dot{v} = -v + y \tag{4.4}$$

$$y = \max(0, x - \theta) \tag{4.5}$$

where v is the inner state of the neuron that represents self-adaptation and τ' is the time constant for the the adaptation.

Fig. 4.1 shows the step response of a neuron with different self-adaptation rates. For

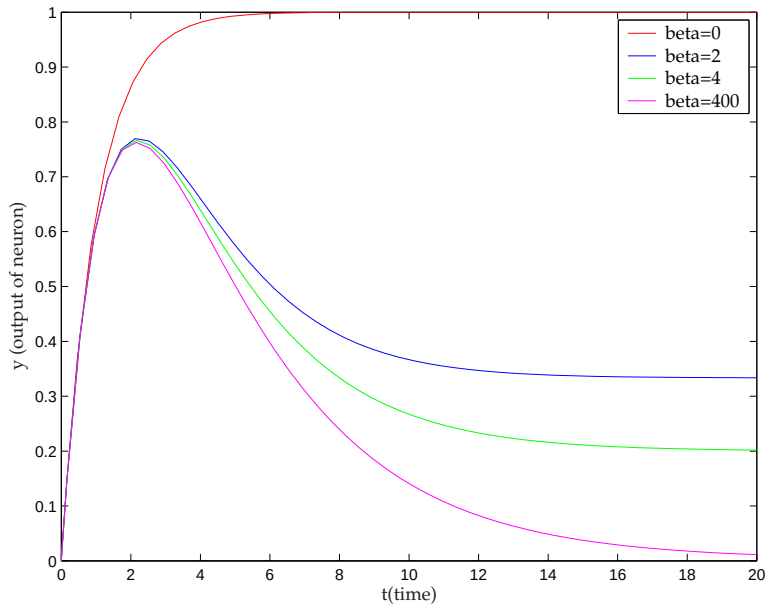

Figure 4.2: Step response of a single neuron with different value of β. for all curves, $\tau = 1$, and $\tau'/\beta = 5$

$\tau' = 10$ and $\tau' = 8$, the firing rate of the neuron is an over-damped response. And $\tau' = 4$ and $\tau' = 2$ result in an oscillation. Considering the actual biological neuron doesn't display such an oscillation, it should be avoided when the parameters of the neuron are to be decided.

To ensure that the firing rate of the neuron doesn't oscillate with a step stimuli, following condition has to be satisfied:

$$(\tau' - \tau)^2 \geq 4\tau'\tau\beta \tag{4.6}$$

Another issue to be noted is that when β is small (with a constant τ'/β) the neuron is more subject to the constant input than the changing input (low-pass filter). Step responses of various β is shown in Fig. 4.2. In the extreme case that $\beta = 0$, the self-adaptation effect disappears and the model becomes Morishita's neuron model.

4.1.2 Mutually Inhibiting Network

Now we discuss a mutually inhibiting network that composes of i neurons, with introduction of mutual inhibition between neurons, the single neuron model can be modified slight as below. For simple of discussion, let $\theta = 0$ and τ = 1 thus $x_i - \theta$ and τ'/τ are replaced by x_i and T:

$$\dot{x_i} = -x_i + \sum_{j=1}^{n} w_{ij} y_j + u_i - \beta v_i \tag{4.7}$$

$$T\dot{v_i} = -v_i + y_i \tag{4.8}$$

$$y_i = g(x_i) = \max(0, x_i) \tag{4.9}$$

where w_{ij} ($i \neq j$) is the strength of inhibitory connection from the output of jth neuron to ith neuron and is always positive. u_i is a constant positive input to the ith neuron from outside the network and $\sum w_{ij} y_j$ represents the total input to the ith neuron from other neurons within the network.

Several basic characteristics of the neuron model shown as Eq.(4.7)-(4.9) are defined [Matsuoka (1985)]. These properties ensures the stability of oscillatory solutions for the neuronal networks composes of multiple neurons shown above.

For Eq.(4.7)- (4.9), there exists a unique and bounded solution for any initial state where t $\geq$ 0.

To prove the boundedness, solving Eq. (4.8) with respect to v_i gives

$$v_i(t) = v_i(0)e^{-t/T} + 1/T \cdot e^{-t/T} \int_0^t g(x(u))e^{u/T} du \tag{4.10}$$

Since $g(x) = \max(0, x_i)$ and is non-negative,

$$v_i(t) \geq -|v_i(0)| \tag{4.11}$$

Solving Eq. (4.7) with respect to x_i gives

$$x_i(t) = x_i(0)e^{-t} + u_i(1-e^{-t})$$

$$-\beta e^{-t} \int_0^t v_i(u)e^u du - \sum_j w_{ij} e^{-t} \int_0^t g(x_k(u))e^u du \tag{4.12}$$

Applying Eq.(4.11) to Eq. (4.10), we obtain

$$x_i(t) \leq |x_i(0)| + u_i + \beta|x_i'(0) \mid (1 - e^{-t}) \tag{4.13}$$

thus the upper bound of x_i is obtained:

$$x_i(t) \leq |x_i(0)| + u_i + \beta|v_i(0)| \tag{4.14}$$

Similarly, apply Eq.(4.14) to Eq.(4.10)

$$v_i(t) \leq |v_i(0)| + |x_i(0)| + u_i + \beta|v_i(0)| \tag{4.15}$$

and applying Eq.(4.14) and Eq.(4.15) to Eq.(4.13) we can obtain the lower bound of x_i

$$x_i(t) \geq -|x_i(0)| - \beta(|v_j(0)| + |x_i(0)| + \beta|v_i(0)|)$$

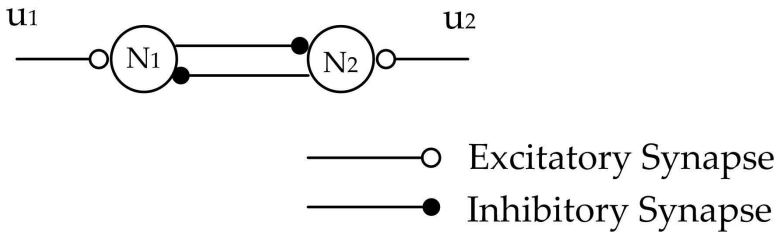

Figure 4.3: Mutual inhibition network with two neurons suppress each other

$$-\sum_{j}(w_{ij}(|x_j(0)| + u_i + \beta|v_j(0)|) \tag{4.16}$$

From Eq.(4.14) and Eq.(4.16) the boundedness of the neuron model is proved.

4.1.3 Neural Oscillator of two-neuron network

Now we consider a mutually inhibited network consisting of two neurons(Fig. 4.3).

$$\tau\dot{x_i} = -x_i + w_{ij}y_j + u_i - \beta v_i \tag{4.17}$$

$$\tau'\dot{v_i} = -v_i + y_i \tag{4.18}$$

$$y_i = \max(0, x_i) \tag{4.19}$$

where $i = 1, 2$ and $j = 2, 1$ for ith neuron.

Matsuoka (1987) has investigated the mathematical condition for the network to produce a stable rhythmic oscillation. By further extending the boundedness of the single neuron model proved in previous section to a coupled neuronal network. The conditions of sustained oscillation are given in the following inequations:

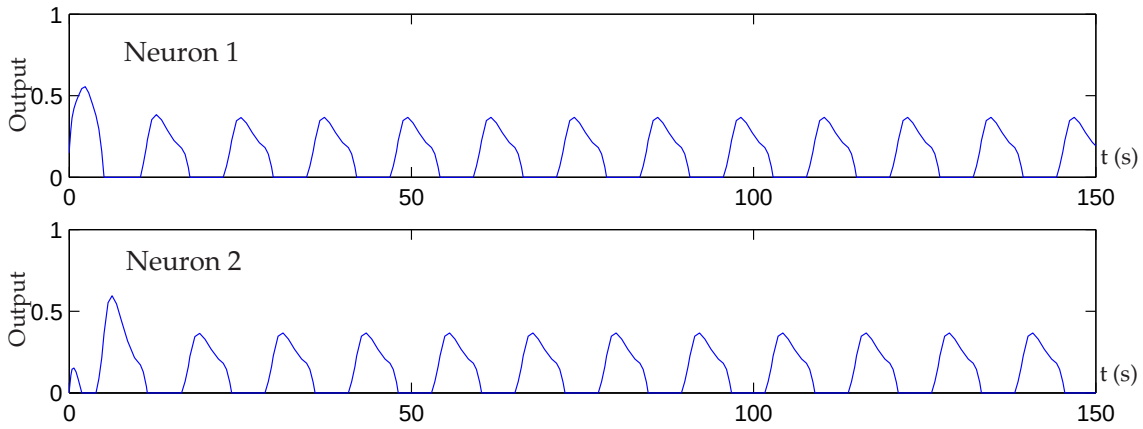

Figure 4.4: Output of each neuron of the network, $\tau = 1$, $\tau' = 10$, $\beta = 5$ and $u_1 = u_2 = 1$ and $w_{12} = w_{21} = 2$

$$w_{12}/(1+\beta) \leq (u_1/u_2) \quad and \quad w_{21}/(1+\beta) \leq (u_2/u_1) \tag{4.20}$$

$$\sqrt{w_{12} \cdot w_{21}} \geq 1 + \tau/\tau' \tag{4.21}$$

These conditions imply a large adaptation rate β is necessary for the rhythmic oscillation. If $\beta = 0$ any w_{12} and w_{21} will not satisfy the above conditions. The large mutual inhibition defined by w_{12} and w_{21} and the threshold function govern the network so that only one neuron can fire at a time and the alternation of firing neuron is caused by the adaptation in the active neuron and the recovery of the dormant neuron because of the decay of the inhibition from the active neuron (Fig. 4.4)

The frequency of the oscillation depends on the values of parameters τ, τ', w_{12}, w_{21} and β. Fig. 4.5 shows the various neuron activities with different parameters. It can be observed that the oscillation frequency has a positive correlation to the adaptation rate β and negative correlation to the time constant of neuron τ, time constant of adaptation τ' and synaptic weight of mutual inhibition w_{12} and w_{21}.

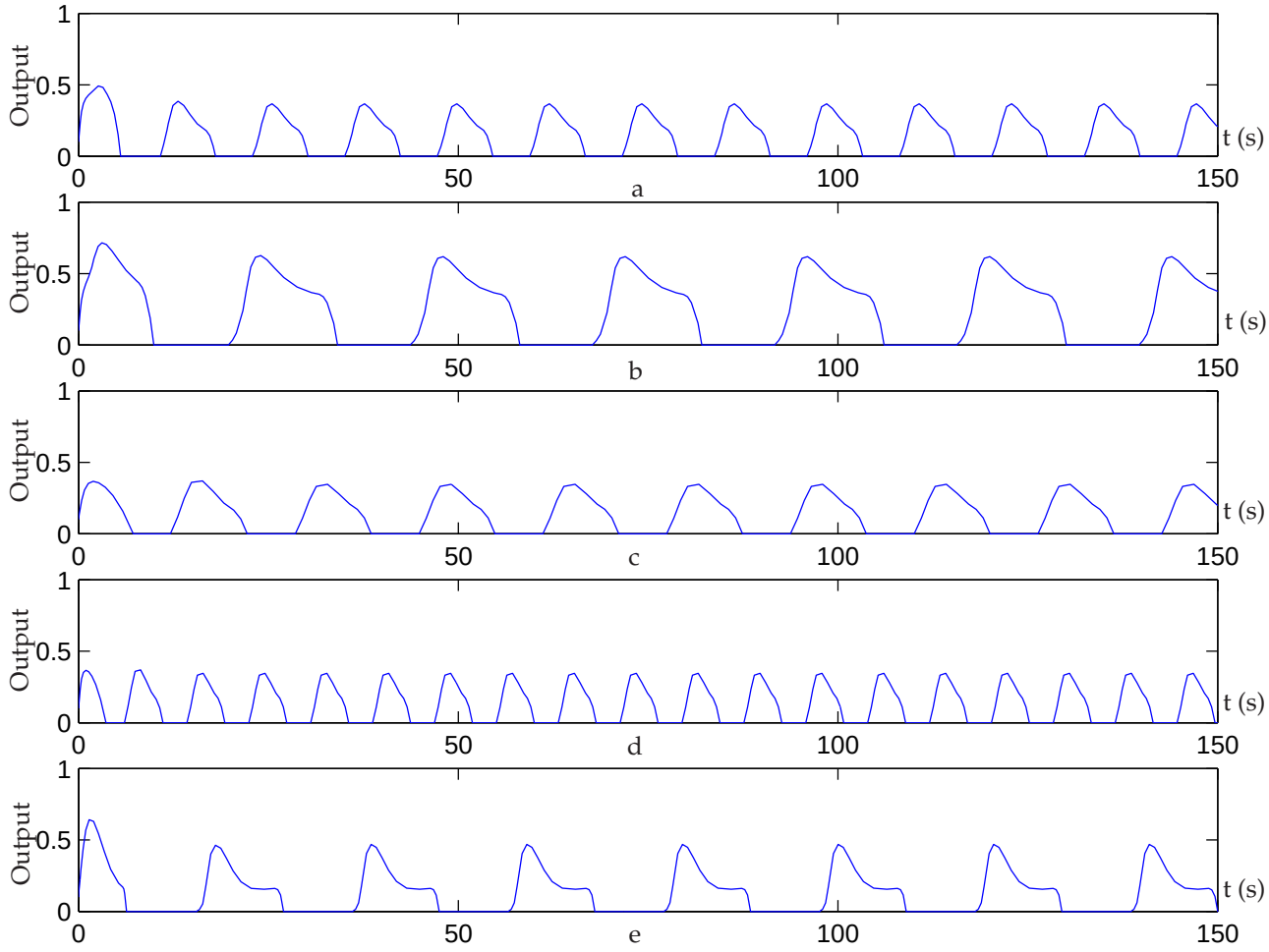

Figure 4.5: Output of neuron 1 with various parameters, similar output can be obtained for neuron 2. **a:** $\tau = 1$, $\tau' = 10$, $\beta = 5$ and $u_1 = u_2 = 1$, $w_{12} = w_{21} = 2$. **b:** all parameters are the same as **a** except $\beta = 2$. **c:** all parameters are the same as **a** except $\tau = 2$. **d:** all parameters are the same as **a** except $\tau' = 5$. **e:** all parameters are the same as **a** except $w_{12} = w_{21} = 4$

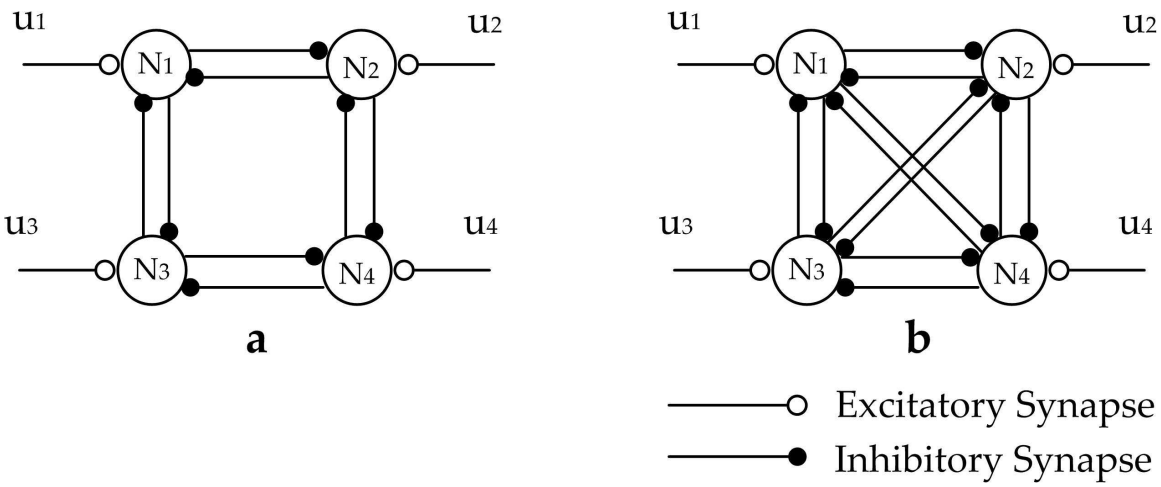

Figure 4.6: Two types of four-neuron network. **a:** bilaterally symmetric network. **b:** completely symmetric network

This two-neuron network is the most simple mutually inhibited network that could generate oscillatory rhythmic pattern. And because the property it displayed resembles the neural activities in real biological world, it is widely accepted as a basic model of neural oscillator (NO) for the muscle activities during locomotion. The two neurons governs the flexor and extensor muscle activity respectively and are often referred to as flexor neuron and extensor neuron.

4.1.4 Four-neuron Network

Now we discuss mutually inhibited networks consisting of four neurons. Depending on the synaptic connections, two different networks can be organized (Fig 4.6).

For network **a**, the sufficient condition for stable rhythmic oscillation can be obtained similarly as the two-neuron network:

$$\sum_j w_{ij} u_j / (1 + \beta) \leq u_i \tag{4.22}$$

$$\sqrt{w_{ij} \cdot w_{ji}} \geq 1 + \tau/\tau' \tag{4.23}$$

where $i = 1 - 4$, $j = 1 - 4$ and $i \neq j$

Matsuoka (1987) introduced the so-called structurally unstable network. Letting ***SUB*** be a subset of neurons of a network. A ***SUB*** has no synaptic connection within it and every neuron beyond ***SUB*** has at least one synaptic connection with neurons within ***SUB***. If there is no ***SUB*** in a network, it is thus called a structurally unstable network.By this definition, network **a** doesn't belong to the structurally unstable network, for we can easily find two ***SUB***s: SUB_1 = {N_1, N_3} and SUB_2 = {N_2, N_4}. This gives a sufficient condition for sustained oscillation for mutually inhibited network consists of any number of neurons.

Network **b** on the other hand, by definition is a structurally unstable network. For a structurally unstable network, the rhythmic oscillation can be evoked even without adaptation given that the synaptic connection is strong. In this case, the alternation of firing neurons is primarily governed by the inter neuron inhibitions rather than the adaptations of the individual neurons.

Both networks **a** and network **b** can be treated as network with two NOs and in network **a**, each type of neuron (either *flexor neuron* or *extensor neuron*) are inhibited by the same type of neuron from the other NO, while in network **b**, both types of neurons are inhibited by each other reciprocally. Since in biological world, different types of neurons from different NO are not strongly correlated with each other, for practical consideration, network **a** is more suitable for modeling neural activities of locomotion.

4.2 Other Neural Oscillator Model

Except the Matsuoka model, another widely accepted NO model is based on Van der Pol oscillators [Dietz (2003)]. Each Van der Pol Oscillator form a neuron which displays certain oscillatory behavior, and synaptic connections among oscillators forms the coupling of the CPG.

4.2.1 Single Van der Pol Neural Oscillator

The oscillator is described by the well-known Van der Pol equation

$$\ddot{x} - \mu(\rho^2 - x^2)\dot{x} + g^2 x = 0 \tag{4.24}$$

From Fig.4.7 we can see that compared to the Matsuoka NO where the neuron has only positive output when it is firing and zero output when it is at rest, the output of Van der Pol NO has both positive and negative values which oscillates in a continuous manner. This is because the output in the Van der Pol NO is a summation of both flexor and extensor neurons, which behaves in a completely opposite manner. The Matsuoka NO will produce a similar sinusoidal oscillation pattern as well if we sum up the output of extensor neuron with a positive value and the output of flexor neuron with a negative value.

Different from Matsuoka NO model, the rhythmic oscillation of Van der Pol Oscillator is inherently stable provided it is not initiated from a stable equilibrium point (***i.e.*** $(x, \dot{x}) = (0, 0)$). This can be observed from the limit cycle behavior shown in Fig. 4.8. The output of the NO always fall into limit cycle within a few seconds regardless of where the initial state of the NO starts from.

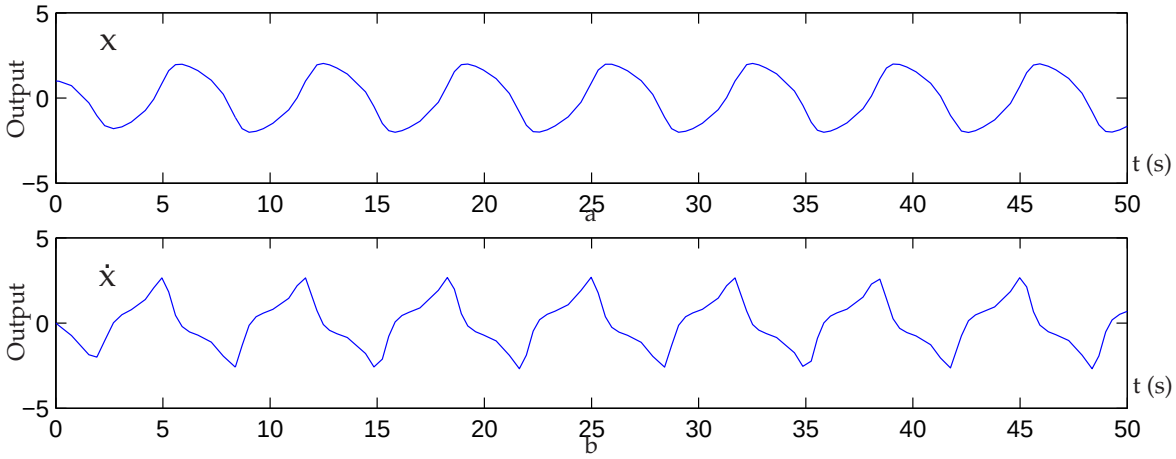

Figure 4.7: Output of a single Van de Pol Oscillator. $\mu = 1$, $g^2 = 1$, $\rho^2 = 1$

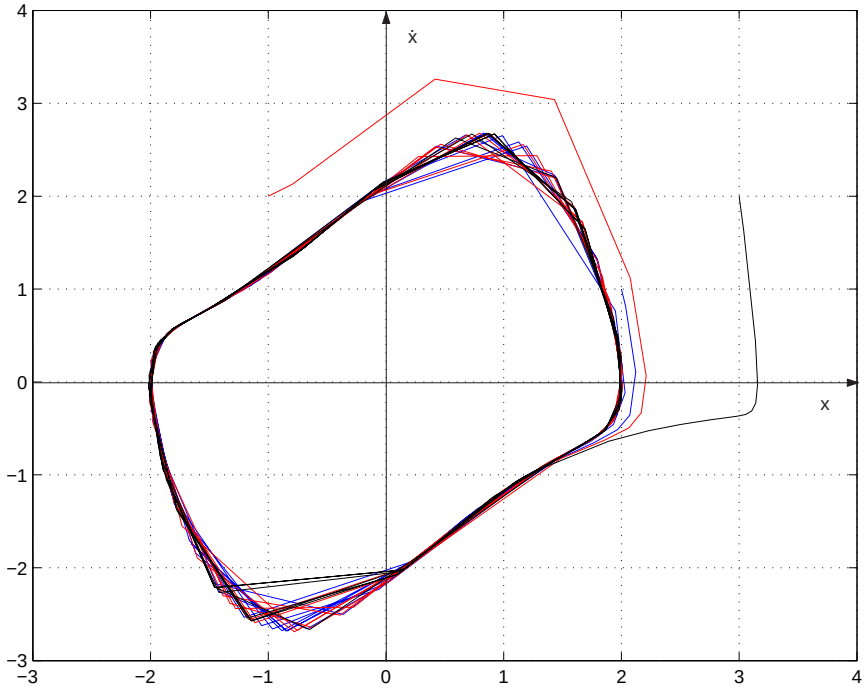

Figure 4.8: The limit cycle behavior of a single Van de Pol Oscillator with various initial conditions: $(x, \dot{x}) = (3, 2), (2, 1) and (-1, 2)$

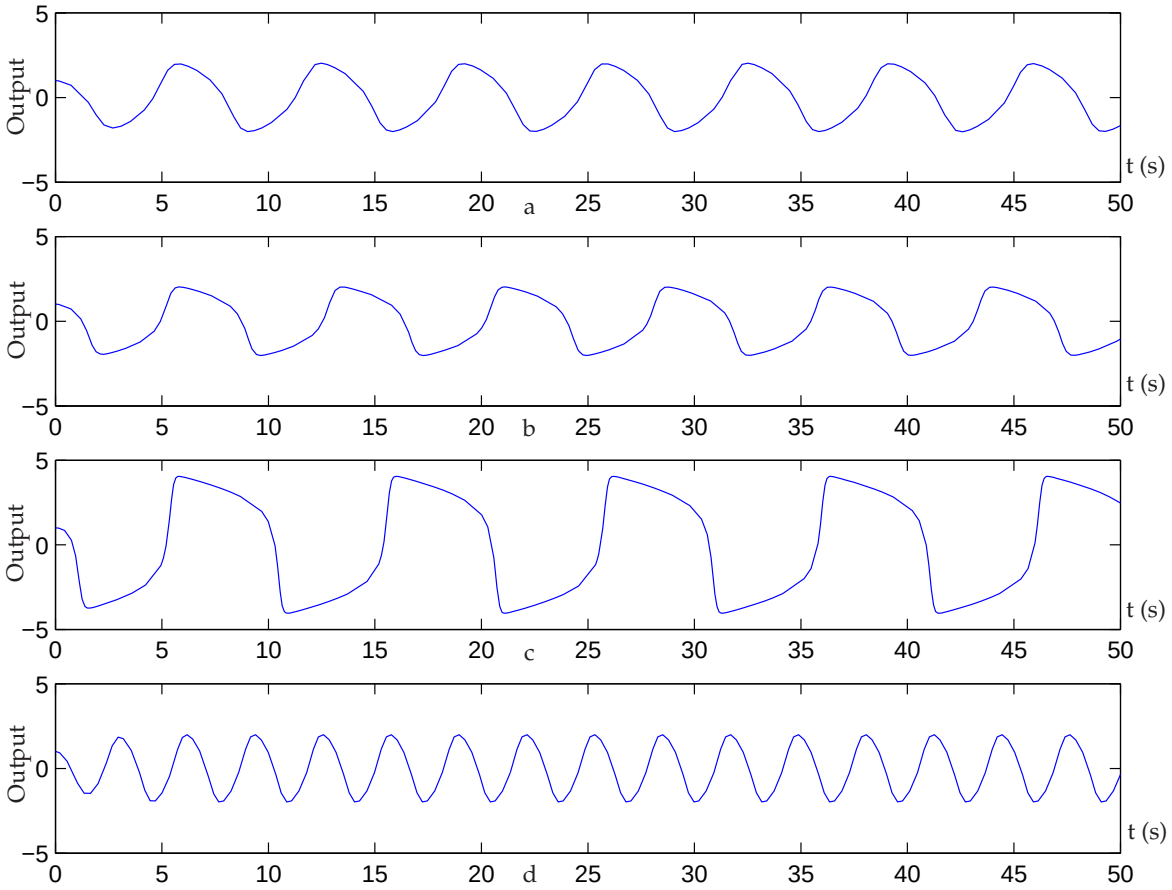

Figure 4.9: **a:** $\mu = 1$, $g^2 = 1$, $\rho^2 = 1$, **b:** all parameters are the same as **a** except $\mu = 2$, **c:** all parameters are the same as **a** except $\rho^2 = 4$, **d:** all parameters are the same as **a** except $g^2 = 4$

The oscillation frequency of the NO output depends on the values of the parameters of the NO as well. Fig. 4.9 shows the rhythms generated from different parameters. It can be observed that the oscillation frequency has a strong negative correlation with ρ^2 and weak negative correlation with μ and it is positively correlated with g^2. In addition, increase of ρ^2 will give rise to an increased oscillation amplitude as well while changing the value of μ and g^2 doesn't affect the amplitude of oscilliation significantly.

The inherent oscillatory property of Van der Pol NO displayed in Fig. 4.9 has inspired many researchers choosing it as a good candidate as the neuron model to compose com-

plicated networks. Bay and Hemami (1987) first investigated a network with four sets of Van der Pol NOs. After that, many other researchers have successfully adopted Van der Pol to achieve various forms of stable bipedal walking [Willer and Miranker (1993); Jalics et al. (1997)]. A bipedal gait synthesized by CPG of four Van der Pol NO is given in Appendix A.

4.3 Summary

In this chapter we discuss the basic biological principle of locomotion. The concept of Central Pattern Generator (CPG) as a network of Neural Oscillators (NO) is introduced.

Two commonly used mathematical models of neural oscillators (NO) Matsuoka NO and Van der Pol NO are then presented. These two models are commonly utilized to simulate the neural oscillatory activities during animal locomotion.

Although the neural activities in real biological creatures are extremely complicated and these NO models are somewhat primitive comparing with their biological counterparts, these models can still reproduce most of the characteristics of the neural activities such as mutual inhibition and stable oscillatory pattern which are directly relevant to locomotion. It is thus practical to apply these NOs to CPG models that can be utilized for robot locomotion with decent similarity to biological CPG.

Chapter 5

Bipedal Locomotion Control using CPG

In the previous chapter, we present two mathematical neuron models. Properties of various CPG networks with multiple neural oscillators are presented. These CPG display a decent resemblance to the biological neural activities.

In this chapter, we propose a simple architecture to control the locomotion of a bipedal robot by utilizing a CPG network with four neural oscillators (NOs). The CPG network is coupled with sensory feedback from the robot. The feedback makes the CPG and robot entrained with each other. The simulation results suggest our proposed control architecture can generate a smooth and continuous walking pattern for the bipedal robot.

5.1 Global Entrainment of Limit Cycle

A CPG shows a limit cycle behavior. A stable walking pattern should also display a limit cycle of same frequency. However, the robot is a mechanical system with mass and inertia, and the motor command generated by CPG may not be achieved by the robot immediately.

The CPG network shown in previous chapter is isolated CPG with synaptic connections from only within the network. Although it can generate continuous stable walking pattern, there is no sensory information passed on from the robot to the CPG. This is like a biological CPG without afferent neurons. By introducing a feedback pathway, we complete our CPG network model.

The feedback provides a servo mechanism to monitor the actual limb movement against the CPG output. The error signal then comes back to the CPG, updating internal state variables of the individual neuron. In this way, the robot movement is entrained with the limit cycle behavior of the CPG.

5.2 Proposed Control Architecture

In order to achieve stable bipedal locomotion, a general control architecture is proposed. The neural activities generated by CPG network are synthesized as a part of locomotion activity.

In the sagittal plane, a CPG network composed of four neural oscillators (NO) based on Matsuoka neuron model is used to control the hip and knee joints of the robot. The feedback pathway from the robot to the neurons has been introduced to the CPG model. This results in a global entrainment between the rhythmic oscillation of the CPG and the robot dynamics. The ankle pitch joints of the robot are controlled by a posture stablizer to maintain the upright stability of the robot. Fig. 5.1 shows the sagittal control architecture.

To simply our discussion, no CPG is imposed in the frontal plane. Instead, we apply a servo mechanism to maintain the lateral stability. A PD controller is used at ankle and hip roll joints to prevent the robot from tipping over to the side during the walking cycle.

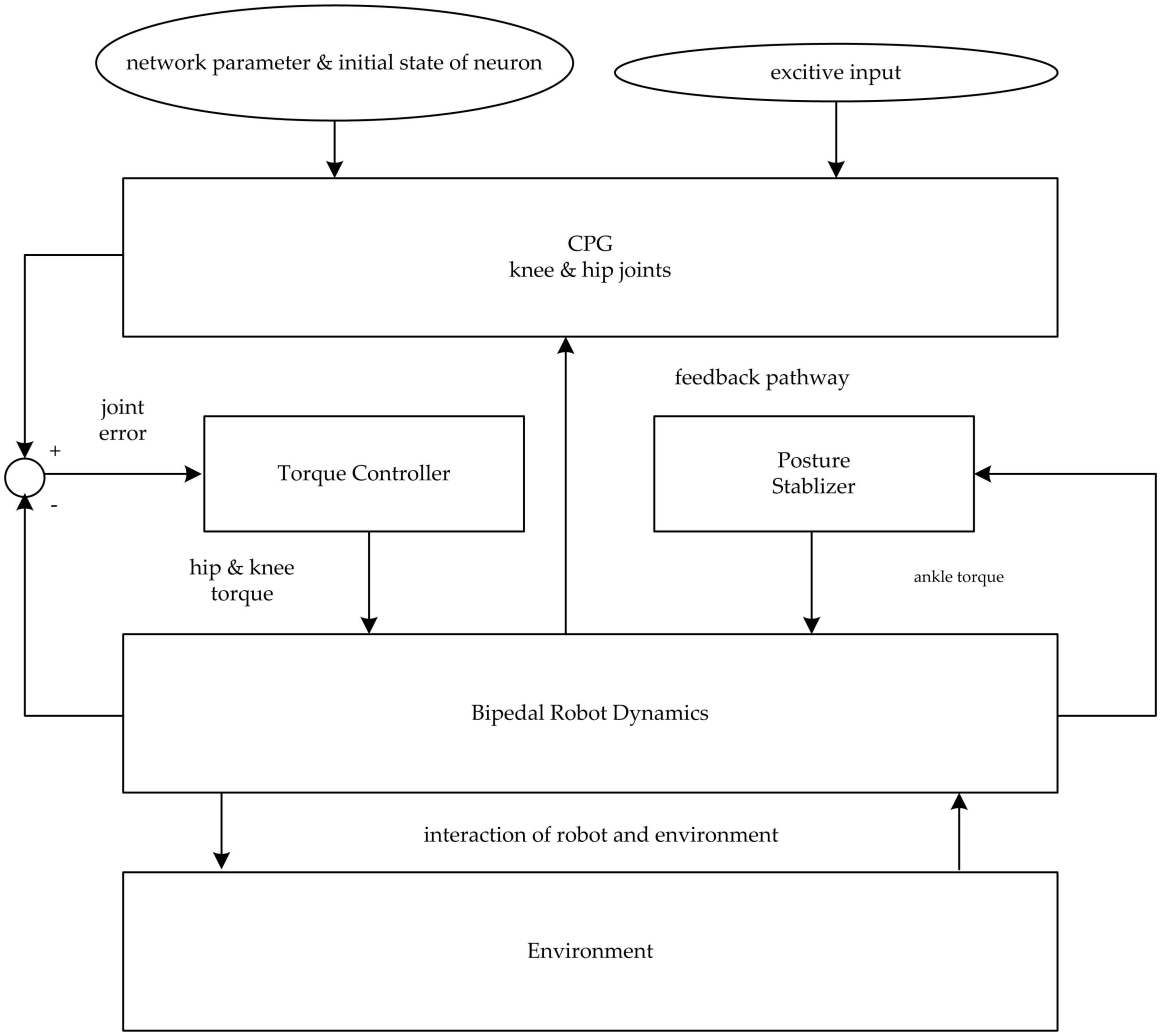

Figure 5.1: Proposed control architecture in the sagittal plane for the bipedal robot

The control architecuture we propose here has following properties:

- The three dimensional walking is decoupled into sagittal plane and frontal plane. The rhythmic oscillatory pattern of neurons generated by the CPG is feedforward to the hip and knee joints in the sagittal plane of the robot by the torque controller. In the frontal plane, a simple servo mechanism with high gain PD controller is applied.
- The global entrainment of CPG and the dynamics of the robot is realized through the feedback pathway from the the robot to the CPG. In the presence of this feedback, the neural activities generated by the CPG network is adjusted according to the robot kinetic and dynamic conditions on the real-time basis.
- The derivation of mathematical model of the robot is not necessary. The stability of the locomotion is fully governed by the the stability of limit cycle behavior of the CPG through global entrainment given that the parameters of the CPG and feedback is properly chosen.

5.3 CPG network of four NOs

The CPG network (Fig.5.2) we discuss here utilizes four NOs. Each NO consists of two Matsuoka neurons (flexor and extensor neurons). The mathematical functions of neurons are given as below:

$$\begin{aligned}\tau_i \dot{u}_{\{e,f\}i} = &-u_{\{e,f\}i} - \beta v_{\{e,f\}i} - w_{ef} y_{\{f,e\}i} \\ &- \sum_{j=1}^{n} w_{ij} y_{\{e,f\}j} - feed_{\{e,f\}i} + u_0 \end{aligned} \tag{5.1}$$

$$\tau_i' \dot{v}_{\{e,f\}i} = -v_{\{e,f\}i} + u_{\{e,f\}i} \tag{5.2}$$

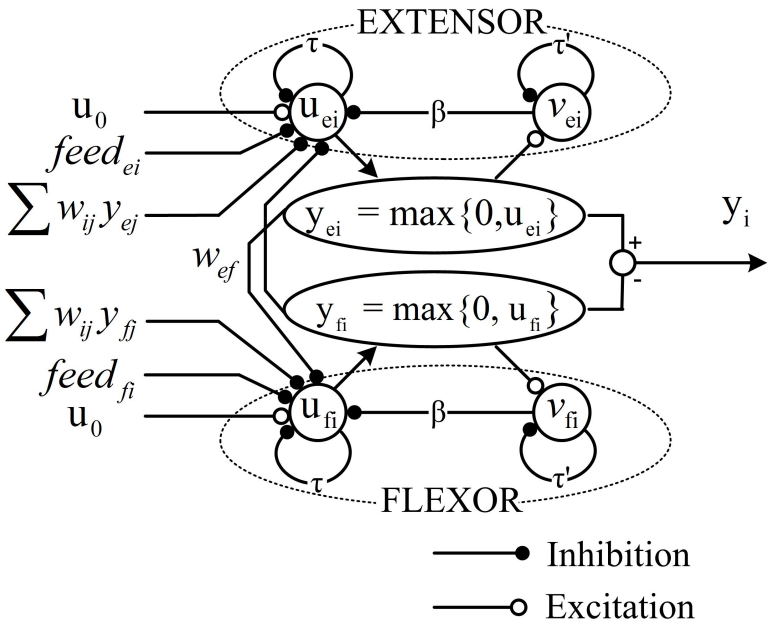

Figure 5.2: A Neural Oscillator with two mutual inhibiting neurons. For the CPG network discussed here, four NOs are interconnected to control the hip and knee joint of the bipedal robot in Sagittal plane

$$y_{\{e,f\}i} = \max\{0, u_{\{e,f\}i}\} \tag{5.3}$$

where $u_{\{e,f\}i}$ is the membrane potential of the ith ($i = 1 - 4$) extensor or flexor neuron. and $v_{\{e,f\}i}$ is the state variable that defines self-adaptation of the neuron. β defines the rate of self-adaptation.u_0 is the external excitive input with a constant rate which initiates the oscillatory activity of the neuron and maintains it at a certain level. τ_i and τ_i' are time constant of the membrane potential and the self-adaptation of the neuron. w_{ef} is the connecting weight of the extensor neuron and flexor neuron within a NO and w_{ij} is the the connecting weight of cross-NO inhibition from neuron of the jth oscillator.

$y_{\{e,f\}i}$ is the output or firing rate of each neuron within the NO. It triggers the movement of either the extensor muscle or the flexor muscle.The summation y_i is defined as the output of the NO (see Fig. 5.3).

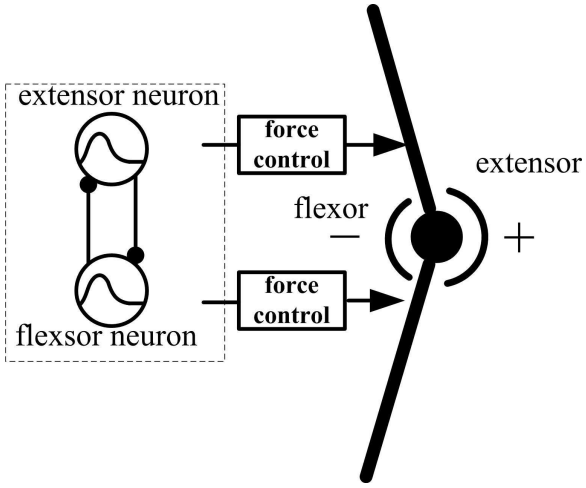

Figure 5.3: A single joint controlled by neural oscillator

$feed_{\{e,f\}i}$ is the term which defines sensory feedback from the robot. It is organized such that it adjusts the temporal neuron activities of the CPG without overriding its rhythmic oscillation. The feedback is a function of inertial angles and angular velocities of joints. The inhibitive feedback makes the CPG entrained with the dynamic system of the robot. Details of the sensory feedback are discussed in Subsection 5.5.2.

5.4 The Seven-link Bipedal Robot

In order to test the proposed control architecture, a seven-link three dimensional bipedal robot is constructed in simulation environment as shown in Fig.5.4. The mass and geometric distribution of each link is shown in Table 5.1.

The robot has a total of ten DOFs. For each leg, two DOFs (pitch and roll) are located at each hip, one at the knee (pitch) and two at the ankle (pitch and roll). Each DOF is actuated by a torque generator.

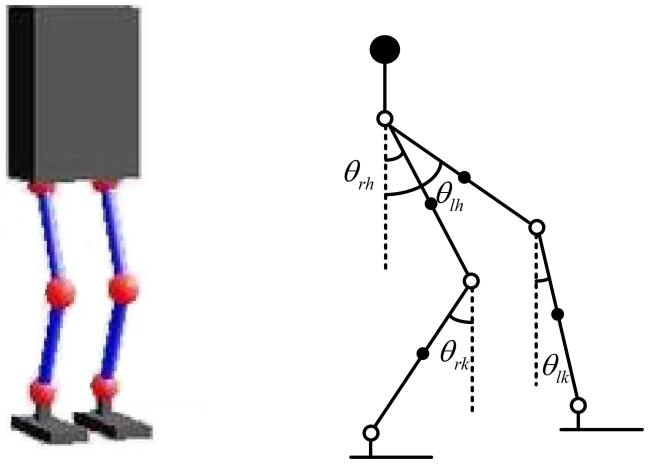

Figure 5.4: Structure of the Bipedal Robot

Table 5.1: Geometric and Mass Distribution of the Bipedal Robot

Link	*Mass*	*Moment of Inertia* (Ixx, Iyy, Izz)	*Length*
Trunk	1.000 [kg]	0.500, 0.050, 0.500 [kgm^2]	0.120 [m]
Thigh	0.400 [kg]	0.005, 0.005, 0.0001 [kgm^2]	0.080 [m]
Shank	0.400 [kg]	0.005, 0.005, 0.0001 [kgm^2]	0.080 [m]
Foot	0.100 [kg]	0.001, 0.001, 0.000075 [kgm^2]	0.075 [m]

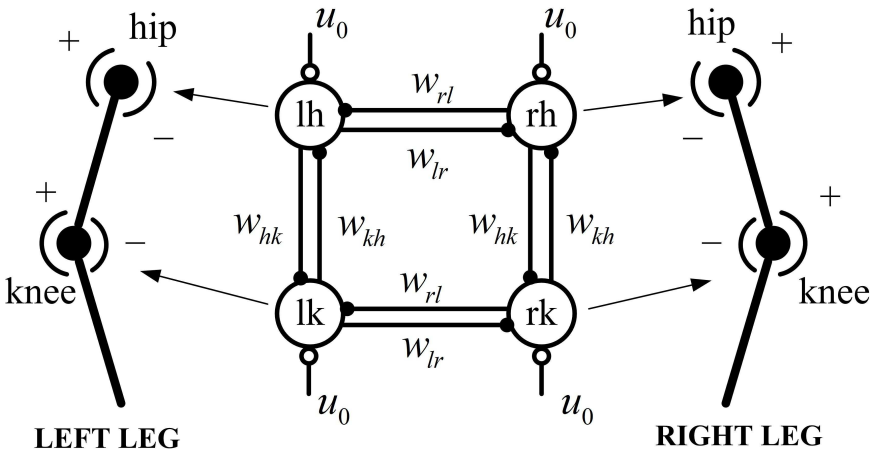

Figure 5.5: CPG-bipedal robot

5.5 Neural-musculoskeletal system

5.5.1 Forward Coupling

The feedforward coupling of the CPG and dynamic system of the robot is established by using the output of CPG directly to control the torque in the respective joints. Our CPG comprises of four NOs described in Eq.(5.1)-(5.3) controlling the hip and knee pitch joints of each leg as shown in Fig.5.5. The control of ankle pitch joints are not included in the CPG model. Instead, a posture stability controller is utilized. Four DOFs in the lateral plane is controlled by PD controller to minimize its motion within the plane. The reason CPG is not used for ankle pitch and the posture stability controller are discussed in detail in Subsection 5.5.3

The output of the four NOs is then sent to the torque generator situated at the hip and knee joints.

$$\tau_{\{l,r\}h} = k_{ph}(\hat{\theta}_{\{l,r\}h} - \theta_{\{l,r\}h}) + k_{dh}(0 - \dot{\theta}_{\{l,r\}h}) \tag{5.4}$$

$$\tau_{\{l,r\}k} = k_{pk}(\hat{\theta}_{\{l,r\}h} - \theta_{\{l,r\}h}) + k_{dk}(0 - \dot{\theta}_{\{l,r\}h}) \tag{5.5}$$

$$\hat{\theta}_{\{l,r\}h} = y_{e\{l,r\}h} - y_{f\{l,r\}h} \tag{5.6}$$

$$\hat{\theta}_{\{l,r\}k} = y_{e\{l,r\}k} - y_{f\{l,r\}k} \tag{5.7}$$

where $y_{e\{l,r\}h}$, $y_{f\{l,r\}h}$, $y_{e\{l,r\}k}$ and $y_{f\{l,r\}k}$ are the output of the extensor and and flexor neurons of the hip NO and knee NO.

5.5.2 Sensory Feedback From Robot to CPG

In Section 5.1, we mentioned that sensory feedback $feed_{\{e,f\}i}$ of the ith neuron is essential for the entrainment of CPG and the dynamic system of the robot.

Here in this thesis, we choose the feedback to be function of displacements of the respective joints to their original position at the standing up position as well as the joint velocities. It is activated at the respective joints only when the corresponding leg is in support phase. The feedback can be expressed in the following equations:

$$feed_{\{e,f\}\{l,r\}h} = \{+,-\}(K_{hp}(\theta_{\{l,r\}h} - \theta_{\{l,r\}h0}) + K_{hd}\dot{\theta}_{\{l,r\}h}) \tag{5.8}$$

$$feed_{\{e,f\}\{l,r\}k} = \{+,-\}(K_{kp}(\theta_{\{l,r\}k} - \theta_{\{l,r\}k0}) + K_{kd}\dot{\theta}_{\{l,r\}k}) \tag{5.9}$$

where $\theta_{\{l,r\}h}$ and $\theta_{\{l,r\}k}$ are the current angle of hip and knee. $\theta_{\{l,r\}h0}$ and $\theta_{\{l,r\}k0}$ are the initial hip and knee angle when the robot is standing upright. $\dot{\theta}_{\{l,r\}h}$ and $\dot{\theta}_{\{l,r\}k}$ are the current angluar velocity of hip and knee. The sign of Eq.(5.8)-(5.9) depends on whether it is an extensor feedback or flexor feedback. The physical meaning of the feedback is that

when the knee and hip joints exceed the initial condition, it will generate an inhibitive or excitive input to the flexor or extensor neuron. The feedback makes the CPG entrains with the robot dynamics.

5.5.3 Posture Stability Controller

The ankle pitch joints of the robot are controlled by a local stability controller instead of NOs of the CPG. This is because during the single support phase, the ankle joint of the stance leg tends to be a passive joint which has a direct result in the posture stability. With this philosophy in mind, a posture stability controller is applied to the ankle joint during the single support phase.

$$\tau_{\{l,r\}a} = k_{p1}(\hat{\theta}_{\{l,r\}a} - \theta_{\{l,r\}a}) + k_{d1}(0 - \dot{\theta}_{\{l,r\}a}) \\ +k_{p2}(0 - \theta_{tr}) + k_{d2}(0 - \dot{\theta}_{tr}) \tag{5.10}$$

$$\hat{\theta}_{\{l,r\}a} = \theta_{\{l,r\}h} + \theta_{\{l,r\}k} \tag{5.11}$$

$$\hat{\theta}_{\{l,r\}a} = \theta_{\{l,r\}h} + \theta_{\{l,r\}k} \tag{5.12}$$

$\tau_{\{l,r\}a}$ is the torque applied to left or right ankle joint, depending on which one is current stance leg. $\theta_{\{l,r\}a}$ and $\dot{\theta}_{\{l,r\}a}$ are the current angle and angular velocity values of the ankle joints and $\theta_{\{l,r\}h}$ and $\theta_{\{l,r\}k}$ are the current angle values of the hip joints and knee joints. θ_{tr} and $\dot{\theta}_{tr}$ are the inclination angle and rotational velocity of the trunk.

5.5.4 Lateral Plane Control

The lateral plane control of the robot is quite simple, as it is can be roughly decoupled from the sagittal motion [Chew and Pratt (2004)]. During each support leg exchange, a PD controller is used to keep the motion in lateral plane as small as possible. The controller can be expressed in the following equations:

$$\tau_{\{l,r\}ar} = k_{par}(0 - \theta_{\{l,r\}ar}) + k_{dar}(0 - \dot{\theta}_{\{l,r\}ar}) \tag{5.13}$$

$$\tau_{\{l,r\}hr} = k_{phr}(0 - \theta_{\{l,r\}hr}) + k_{dhr}(0 - \dot{\theta}_{\{l,r\}hr}) \tag{5.14}$$

The gain of the PD controller is chosen by trial and error such that the motion in the frontal plane is minimized.

5.5.5 Joint Limits Movement

A limit of maximum joint angles is imposed on the robot. There are two purpose of having joint angle limits. Primarily the limits ensure that the robot can still maintain stability when CPG generates a walking pattern that can not be realized by the robot without falling down. Second, it prevent the robot from having unnautual limb movement as compared with human. For this simulation the joint limit of the bipedal robot for the hip is set to 30 degrees and the joint limit for the knee is set to 50 degrees prevent the posture becoming unnatural.

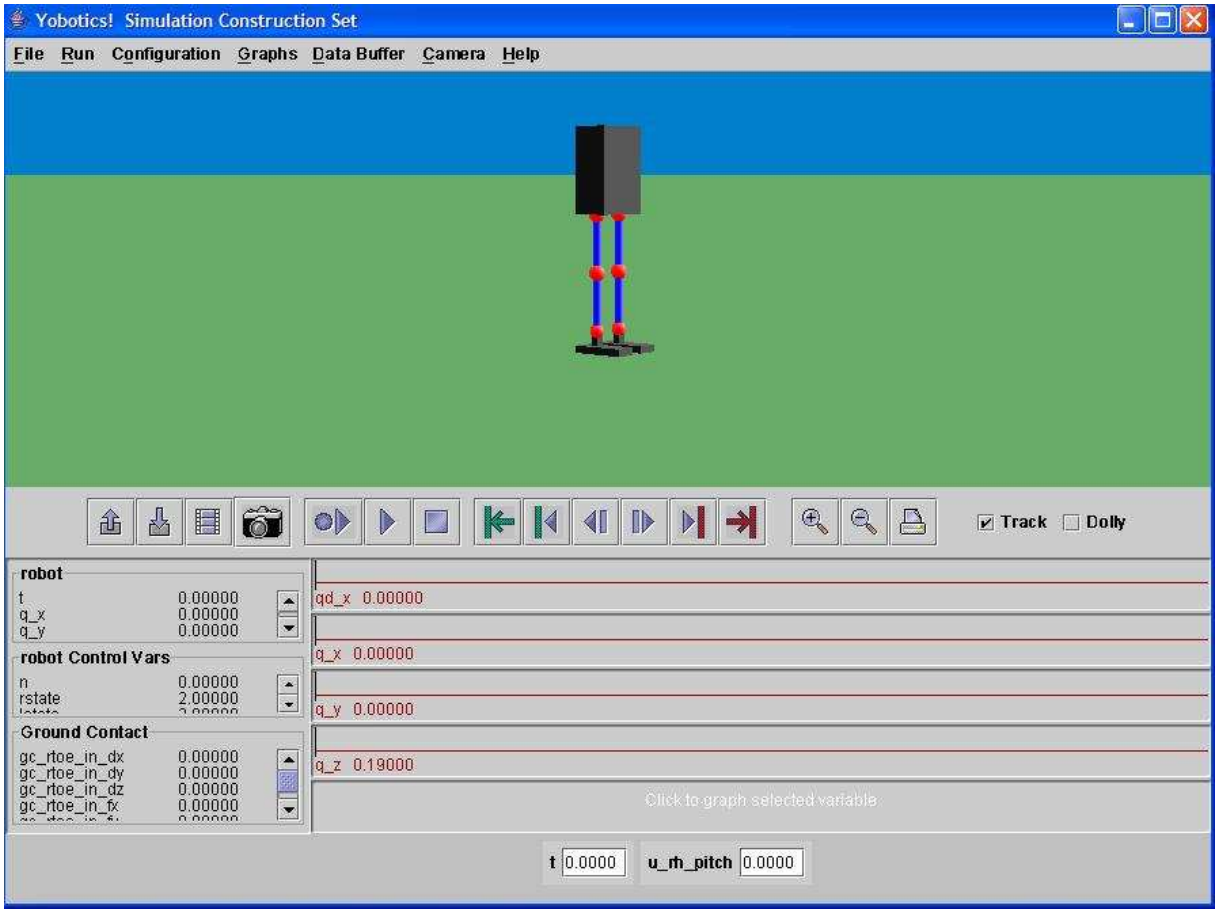

Figure 5.6: Snapshot of Yobotics! simulation environment

5.6 Simulation

Our simulation is carried out in Yobotics! environment. Yobotics! [Yob] is Java package for simulating fully dynamic systems.

The ground is modeled as a spring damper system, with spring and damping coefficient being 40000N/m and 100Ns/m. The time interval T_s of the simulation is 0.5ms.

The key parameters of the CPG is shown in Table 5.2. Parameters of local controllers such as the gains of posture stabilizer and torque controller as well as the high gain PD controller at the frontal plane are shown in Table 5.3

Table 5.2: Key Parameters of the CPG

Parameters	*Value*
Number of NOs	$i = 4$
Excitive input	$u_0 = 5$
Self-adaptation rate	$\beta = 3$
Time constants of neuron	$\tau_i = 0.15$, $\tau_i' = 0.10$
Cross-NO inhibition weight	$w_{hk} = w_{kh} = 1.0$, $w_{rl} = w_{lr} = 2.0$
Inhibition weight within NO	$w_{ef} = 2.0$
synaptic weight of feedback pathway	$K_{hp} = 0.2$, $K_{hd} = 0.2$, $K_{kp} = 0.5$, $K_{kd} = 0.5$

Table 5.3: Parameters of local controllers

Parameters	*Value*
Torque controllers at hip (sagittal)	$k_{ph} = 300$, $k_{dh} = 10$
Torque controllers at knee (sagittal)	$k_{pk} = 20$, $k_{dk} = 0.5$
Posture stabilizer at ankle (sagittal)	$k_{p1} = 50.0$, $k_{d1} = 1.0$, $k_{p2} = 25$, $k_{d1} = 1$
Lateral PD controller at hip (frontal)	$k_{phr} = 100.0$, $k_{dhr} = 1$
Lateral PD controller at ankle (frontal)	$k_{par} = 200.0$, $k_{dar} = 2$

The procedure of the simulation can be itemized as below:

1. Initialize the CPG by setting the parameters in Table 5.2 and the NOs starts the oscillatory activity under external excitive input;

2. Output of the NOs is sent to the torque generator to control the robot;

3. The joint information is acquired and fed back to the CPG through feedback pathway;

4. The updated CPG with sensory feedback is recalculated and the output of the NOs is updated and sent to the torque generator;

5. Repeat 3) and 4) for the next time interval T_s.

5.7 Result and Discussion

Using the parameters shown in Table II and Table III, the bipedal robot is able to walk continuously. Fig.5.7 shows the snapshots of the robot within the first two steps. The movement of the first two steps is a little awkward since the robot is starting from a upright posture and the CPG is trying to entrain with the robot during initial few steps. However our robot managed to maintain posture stability by the the local stability control at the ankle. After three steps the CPG is fully entrained with the robot and a stable global limit cycle begins to emerge.

5.7.1 Neural Activities During Walking

Fig.5.8 shows the neural activities of the CPG in radian when the robot is walking. As we can see the output of NO is jerky at the beginning as it has to overcome the inertia of the whole robot body from zero velocity. But it soon adapts to the walking robot and the oscillation become stabilized. This is due to the sensory feedback from the robot which imposes an entrainment between the robot dynamic system and the CPG.

Fig. 5.9 shows the output of the NOs with different membrane potentials while all the rest of parameters remain the same. We can see that the bigger the u is, the lower the frequency is the frequency of the oscillation. This conforms with the result of isolated CPG shown in previous chapter. Relationship between the neural activities and other parameters presented previously also holds valid in our simulation.

The outputs of the four NOs are directly used to control the torque generators at corresponding joints. Fig.5.10 and Fig.5.11 show the torque generated at the hip joint and knee joint.

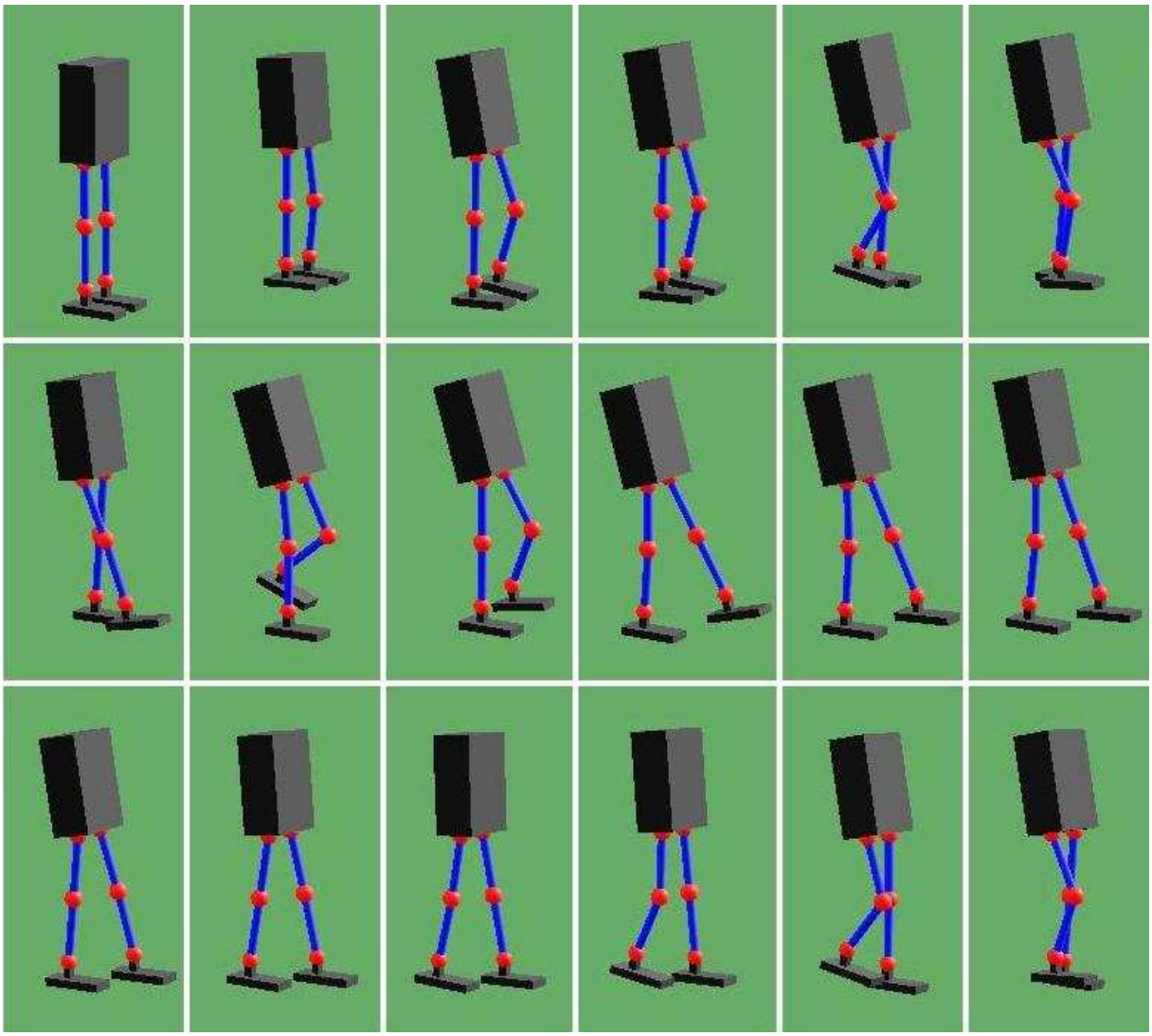

Figure 5.7: Simulation result

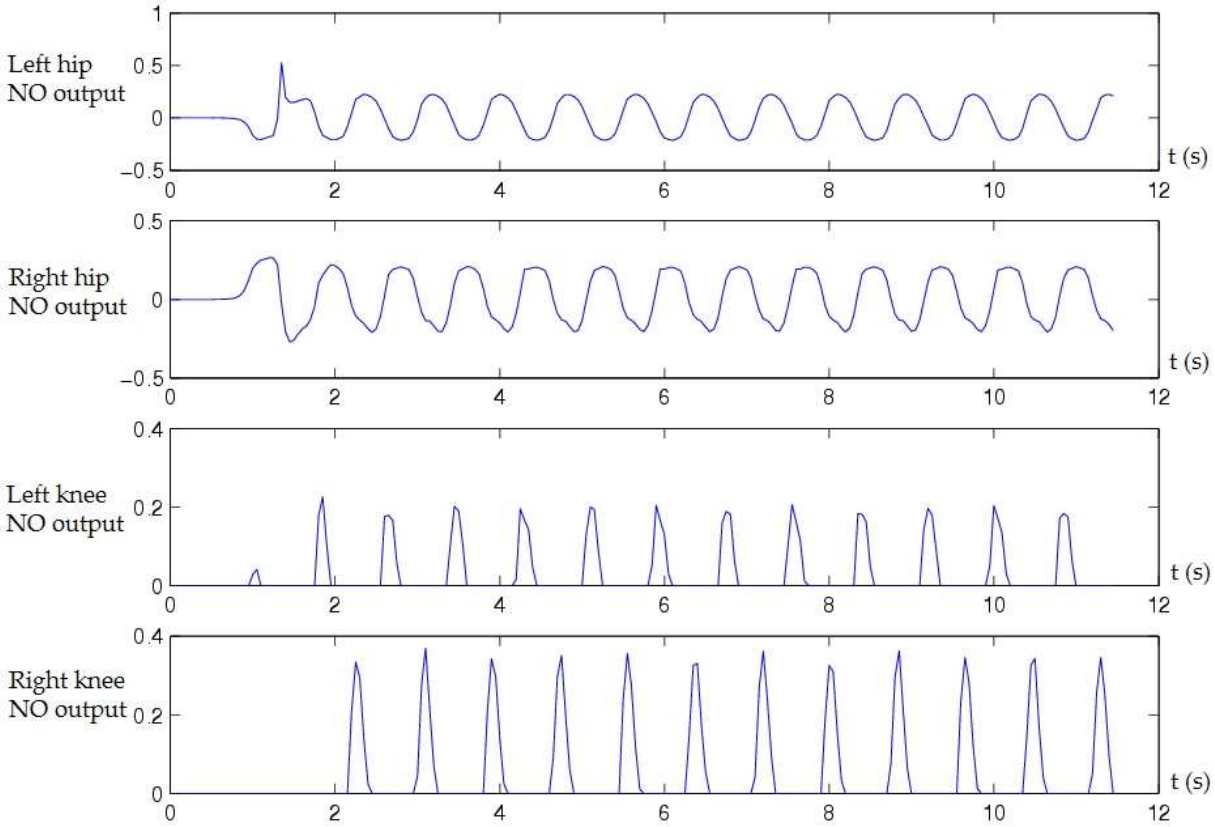

Figure 5.8: Neural activities of the CPG

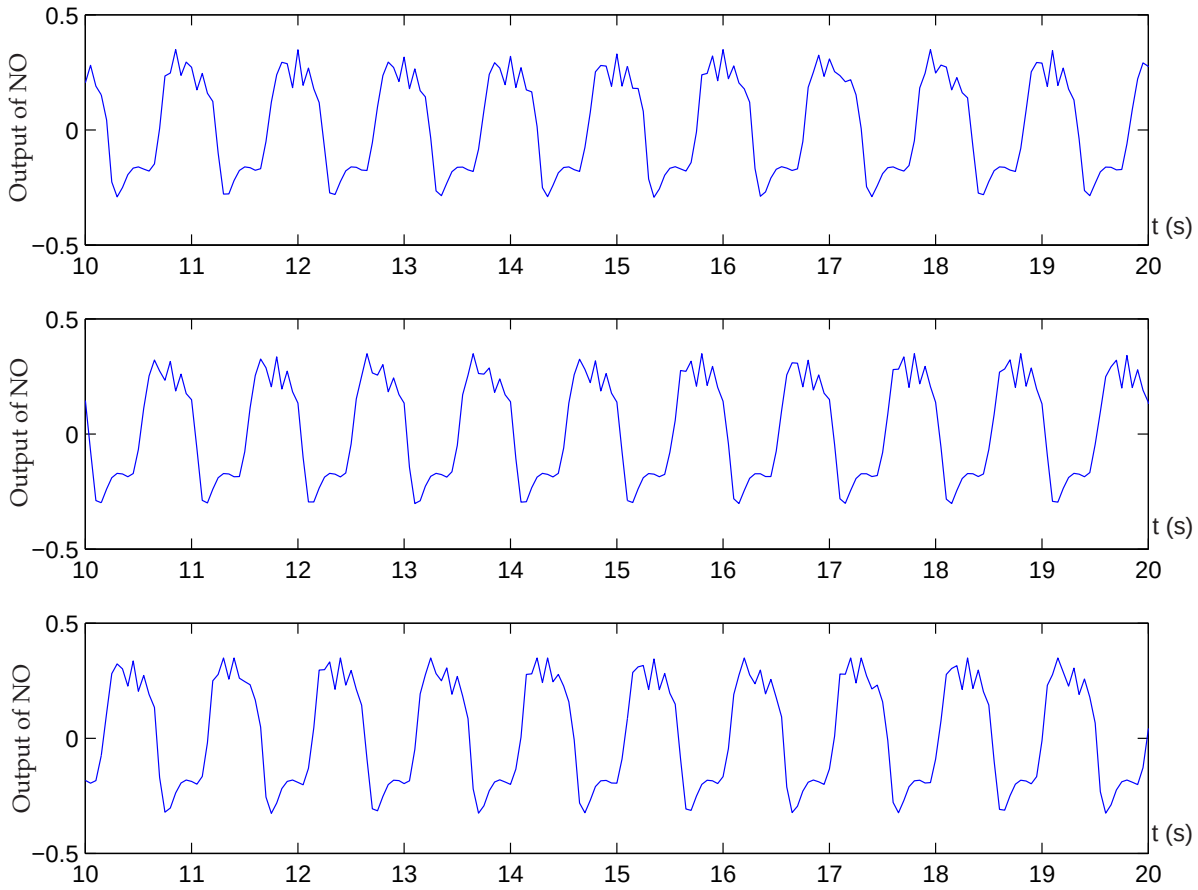

Figure 5.9: NO output with different membrane potentials. From up to down $u = 6$, $u = 5$ and $u = 4$

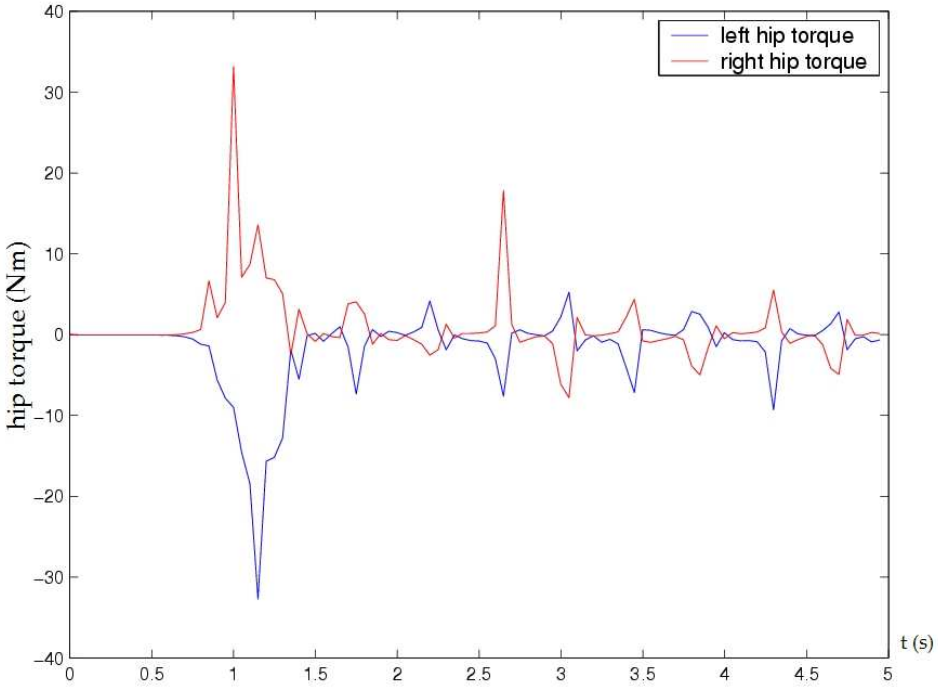

Figure 5.10: Torque generated at hip

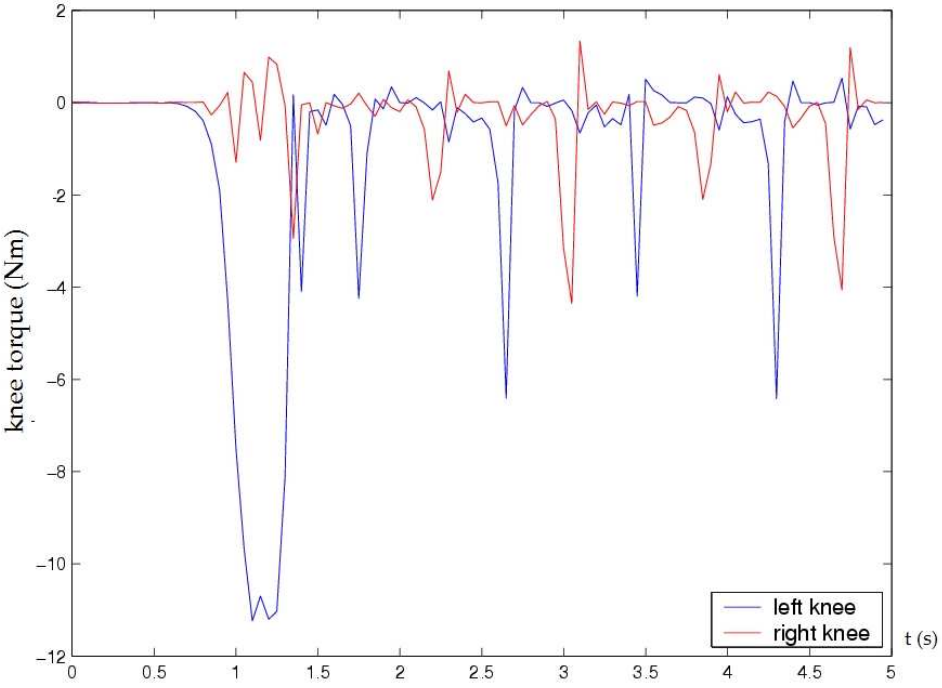

Figure 5.11: Torque generated at knee

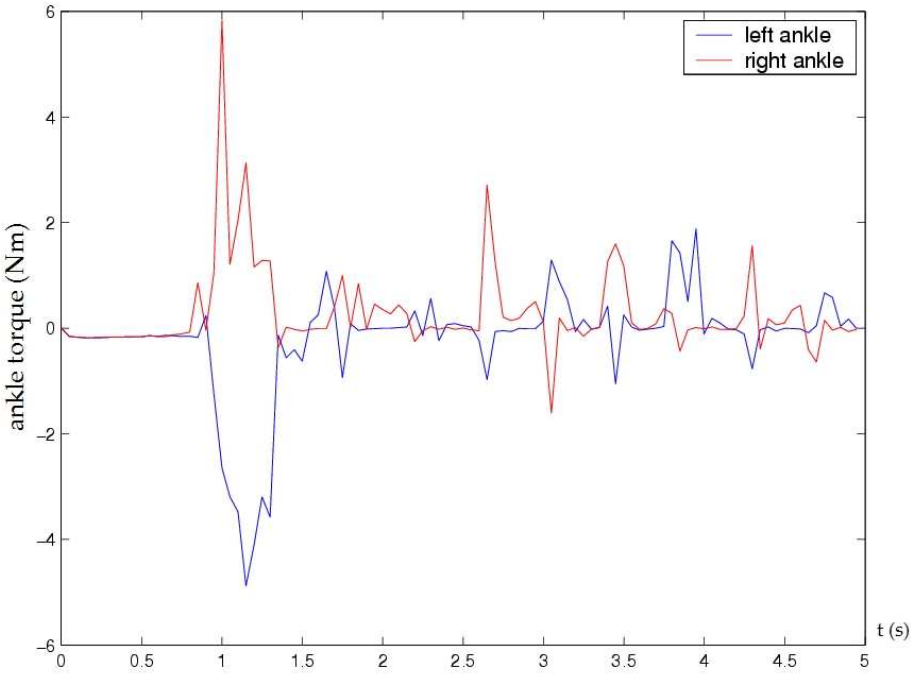

Figure 5.12: Torque generated at ankle

5.7.2 Ankle Joint

As described in the previous section, ankle joint is essential for the posture stability of the robot. Before the CPG generates stable oscillation control signal to the robot, the posture stability is maintained by the local controller at the ankle joint. The torque generated by the stability controller is shown in Fig.5.12. We could notice that there is a sharp increase in both legs during the first step. This is because the robot has to over come its inertia as the walking starts and the walking speed increases from zero velocity.

5.7.3 Limit Cycle Behavior of the Bipedal Robot

Controlled by CPG, a limit cycle behavior is guaranteed given the robot's posture stability is not compromised before the CPG comes to stable oscillation. Fig.5.13 through 5.15 show the angles of each joint.

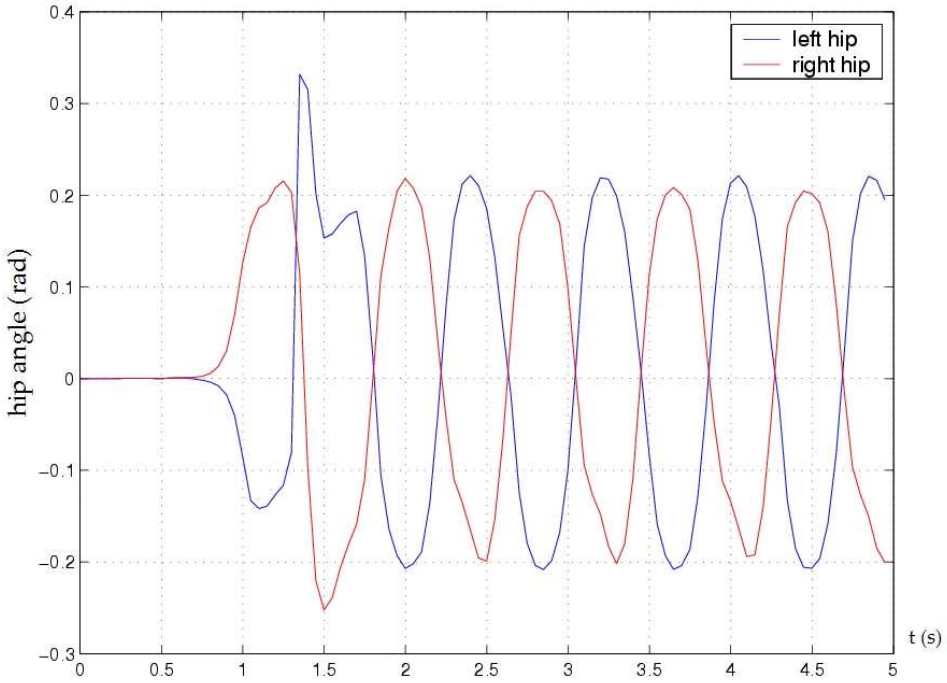

Figure 5.13: Hip joint angles

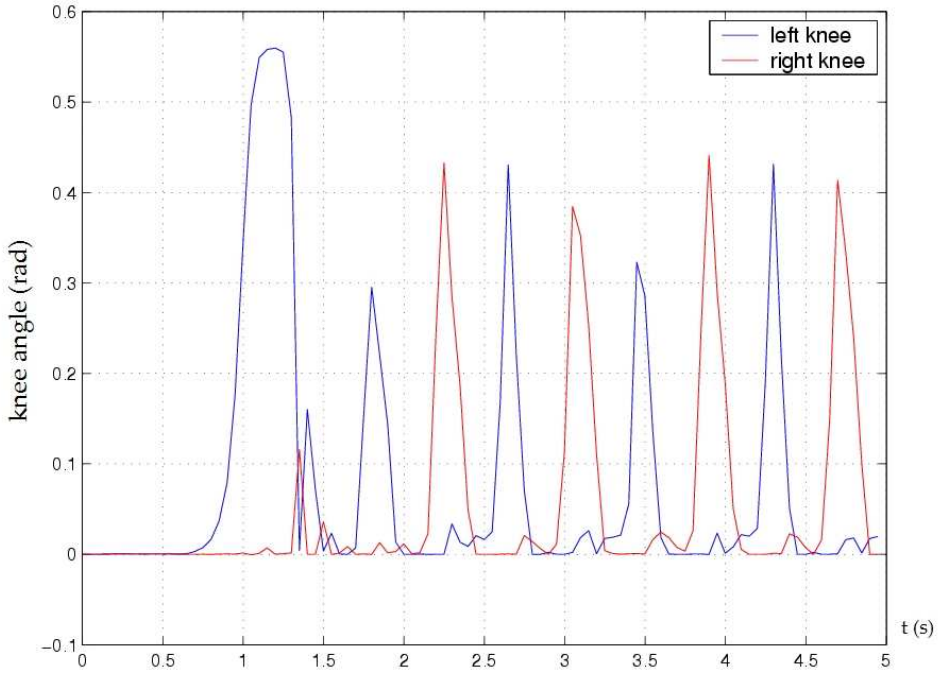

Figure 5.14: Knee joint angles

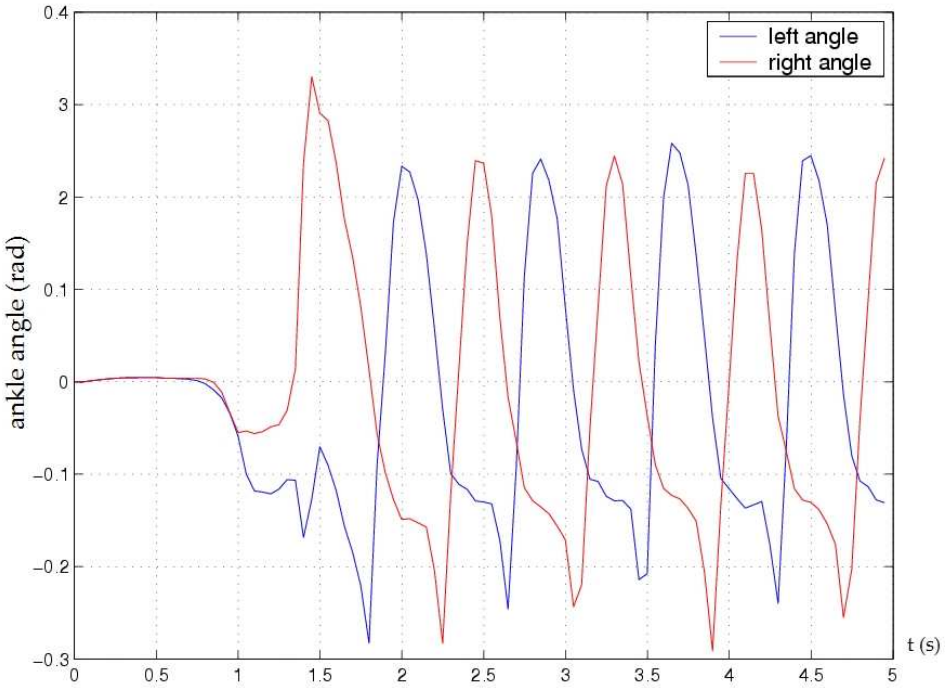

Figure 5.15: Ankle joint angles

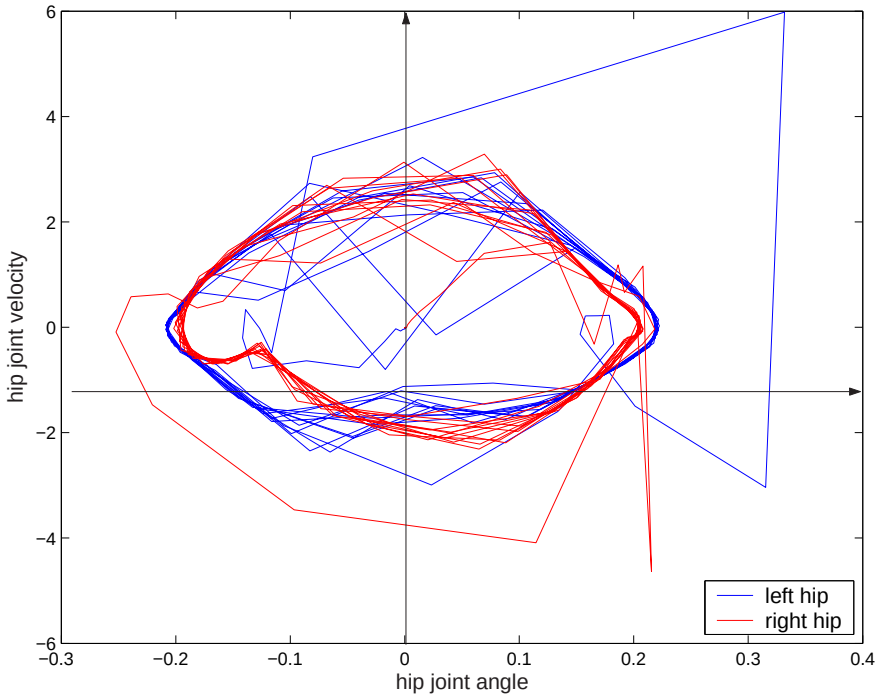

Figure 5.16: Limit cycle behavior of the hip joints

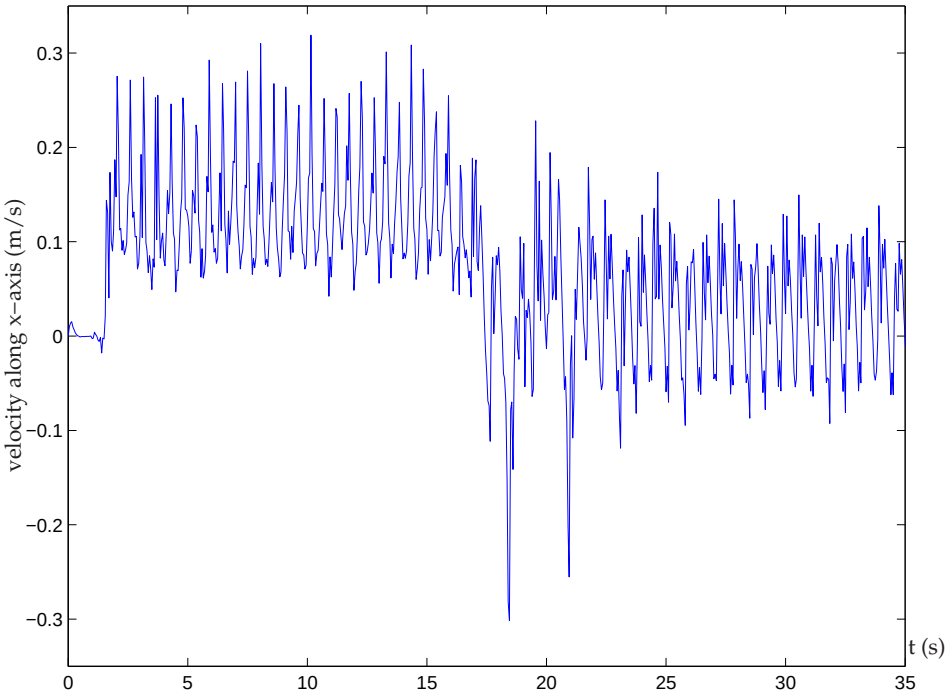

Figure 5.17: Body velocity along the slope

In Fig.5.16, the phase diagrams of the hip joints are plotted. Both left and right hip start from the origin and eventually converge to a constant oscillatory swinging motion. The limit cycle is a result of the entrainment between the CPG and the robot dynamic system. Similar limit cycle behavior can also be identified in knee and ankle joints, although the ankle is not directly controlled by CPG.

5.8 Walking on the Slope

In this section we change the ground condition from the level ground to slope of aproximately 10^o.

We let the robot start downslope first and then immediately upslope. All the parameters of the CPG remain the same as shown in Table 5.2.

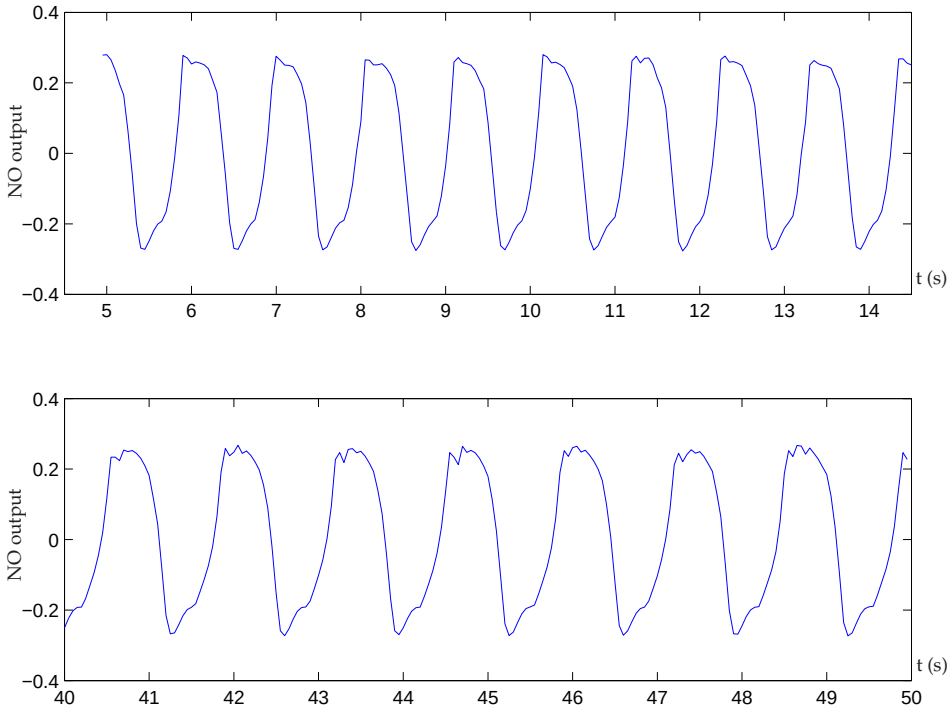

Figure 5.18: Pattern shift from downslope to upslope

The simulation shows a clear global entrainment of robot and CPG. Fig 5.17 is the body velocity alone the slope. When the robot clears the downslope and starts climbing upwards at 15 second, the forward movement of the robot begins to slow down. This velocity change is mainly due to the drop of oscillation frequency as shown in Fig 5.18.

The downslope is easier for robot to walk forward because of gravity. The dynamic of robot is thus taking advantage of this favorible condition and gives a positive feedback to the CPG and the CPG updates its motor pattern accordingly. Likewise when the robot is walking upslope, it is harder for the robot to catch up with the moter command generated by CPG, and as a result, the CPG automatically adjust its oscillation frequency lower. In between the downslope and upslope connections, the velocity appears to be unstabilized, as is shown in Fig 5.17 between 15s to 20s. This is the transitional phase where the CPG is adapting to the new ground condition.

5.9 Summary

In this chapter, we discussed a four-compartmental CPG model and utilized it for locomotion control of a seven-link bipedal robot. The hip and the knee joints are controlled directly by a torque generator by our CPG model to mimic the extension and flexion of the muscle. We applied a posture stability controller to the ankle joint of the stance leg to maintain the stability of the bipedal robot during single support phase. Simulation results indicate that the four-compartment CPG model can successfully generate a walking pattern. And the global entrainment of CPG, the dynamic system of the bipedal robot can be observed from the simulation.

Chapter 6

Conclusion and Future Work

6.1 Conclusion

In this thesis, a bipedal locomotion control strategy after the concept of CPG is proposed. The CPG model utilizes a network of four Matsuoka neural oscillators for motor pattern generation in sagittal plane. Local feedback controllers such as posture stabilizer and lateral movement controller are supplemented to the general control architecture to ensure the robot doesn't tip over or fall side way. Although the CPG model used here is by far a much simplified reproduction of the biological motor control system, the majority of its property is preserved.

The advantages of CPG based control has over other control strategies is its simplicity. In the controller synthesis, no complete or approximated model of the robot dynamics is required. The inherent rhythmic oscillatory pattern of CPG and feedback pathway from robot give rise to a global entrainment between the two. The stable coordinated walking pattern emerges as a result of such entrainment. It even allows the robot to adapt different walking patterns in different environment.

6.2 Discussion of Future Work

A natural extension of the work presented here in this thesis is real life implementation of CPG controlled bipedal robot. The simple model of neurons makes it easy to realize in VLSI circuit. However, concerns mainly come from two aspects:

- Despite the CPG shown in Chapter Five has only four NOs, the system is complicated and so far there is no systematic approach to search for proper parameters for the CPG model. In the simulation, besides the basic conditions of sustained oscillation discussed in Chapter Four, notion of symmetry is also used to confine the search of CPG parameters within a much smaller number candidates. However there is no evidence that asymmetrical CPG will not result in similar sustained rhythmic walking pattern.

- The second issue is the limitation of the hardware actuators. Nowadays, 80% of bipedal robots are actuated by DC motors. As we see in the simulation, the actuation of the bipedal robot is realized through torque generator. Moreover the actuators are constantly interacting with the environment, they require broad bandwidth and high back drivability which DC motors don't have.

If above mentioned issues are well addressed, we are likely to see the CPG based control become a mainstream locomotion control strategy for bipedal robots in the future.

References

URL `http://yobotics.com/simulation/simulation.htm`. Website of the dynamic simulation software Yobotics!

J. Bay and H. Hemami. Modeling of a neural pattern generator withcoupled nonlinear oscillators. *IEEE Trans. Biomedical Engineering*, BME-34:297–306, 1987.

T. G. Brown. The intrinsic factors in the act of progression in the mammal. *Proceedings of Royal Society*, B85:308–19, 1911.

C. Chevallereau, G. Abba, Y. Aoustin, F. Plestan, E.R. Westervelt, C. Canudas-de Wit, and J.W. Grizzle. Rabbit: A testbed for advanced control theory. *IEEE Control Systems Magazine*, October:57–79, 2003.

C. M. Chew and G. Pratt. Frontal plane algorithms for dynamic bipedal walking. *Robotica*, 22:29–39, 2004.

S. Collins, A. Ruina, R. Tedrake, and M. Wisse. Efficient bipedal robots based on passive-dynamic walkers. *Science*, 307:1082–1085, 2005.

V. Dietz. Spinal cord pattern generators for locomotion. *Clinical Neurophysiology*, 114: 1379–1389, 2003.

K. Feng, C.M. Chew, G.S. Hong, and T. Zielinska. Bipedal locomotion control using a four-compartmental central pattern generator. *IEEE International Conference on Mechatronics & Automation*, pages 1515–1520, 2005.

W. O. Friesen and G. S. Stent. Generation of a locomotory rhythm by a neural network with recurrent cyclic inhibition. *Biological Cybernetics*, 18:27–40, 1977.

Y. Fukuoka, H. Kimura, and A. H. Cohen. Adaptive dynamic walking of a quadruped robot on irregular terrain based on biological concept. *International Journal of Robotics Research*, 22:187–202, 2003.

S. Grillner. Neurobiological bases of rhythmic motor acts in vertebrates. *Science*, 228: 143–149, 1985.

K. Hirai, M. Hirose, Y. Haikawa, and T. Takenaka. The development of honda humanoid robot. *Proceedings of IEEE International Conference on Robotics and Automation (ICRA)*, pages 1321–1326, 1998.

Q. Huang, K Yokoi, S. Kajita, K. Kaneko, H. Arai, N. Koyachi, and K. Tanie. Planning walking patterns for a biped robot. *IEEE Tranactions on Robotics and Automation*, 17: 280–289, 2001.

L. Jalics, H. Hemami, and Y. F. Zheng. Pattern generation using coupled oscillators for robotic and biorobotic adaptive periodic movement. *International Conference on Robotics and Automation*, pages 179–184, 1997.

S. Jiang, J. S. Cheng, and J. P. Chen. Design of central pattern generator for humanoid robot walking based on multi-objective ga. *IEEE/RSJ International Conference on Intelligent Robots and Systems (IROS)*, pages 1930–1935, 2000.

S. Kajita and K. Tani. Experimental study of biped dynamic walking. *IEEE Trans. on Control Systems*, Feb:13–19, 1996.

E.R. Kandel, J. H. Schwartz, and T. M. Jessell. *Principles of Neural Science*. McGraw-Hill, 4th edition, 2000.

Q. Li, A. Takanishi, and I. Kato. A biped walking robot having a zmp measurement system using universal force-moment sensors. *International Conference on Intelligent Robots and Systems (IROS)*, pages 1568–1571, 1991.

D. S. Luciano, A. J. Vander, and J. H. Sherman. *Human Functions and Structure*. McGraw-Hill, London, New York, 1978.

K. Matsuoka. Sustained oscillations generated by mutually inhibiting neurons with adaptation. *Biological Cybernetics*, 52:367–376, 1985.

K. Matsuoka. Mechanisms of frequency and pattern control in the neural rhythm generators. *Biological Cybernetics*, 56:345–353, 1987.

T. McGeer. Passive dynamic walking. *International Journal of Robotics Research*, 9:62–82, 1990.

T. A. McMahon. *Muscles,Reflexes, and Locomotion*. Princeton University Press, New Jersey, 1982.

K. Mitobe, Capi G., and Y. Nasu. Control of walking robots based on manipulation of the zero moment point. *Robotica*, 18:651–657, 2000.

S. Miyakoshi, G. Taga, Y. Kuniyoshi, and A. Nagakubo. Three dimentional bipedal stepping motion using neural oscillators -towards humanoid motion in the real world. In *Proceeding of IEEE/RSJ International Conference on Intelligent Robots and Systems (IROS)*, pages 84–89, 1998.

I. Morishita and A. Yajima. Analysis and simulation of networks of mutually inhibiting neurons. *Kybernetik*, 11:154–165, 1972.

K. Nagasaka, Y. Kuroki, S. Suzuki, Y. Itoh, and J. Yamaguchi. Integrated motion control for walking, jumping and running on a small bipedal entertainment robot. *Proceedings of*, pages 3189–3194, 2004.

Y. Okumura, T. Tawara, K. Endo, T. Furuta, and M. Shimizu. Realtime zmp compensation for biped walking robot using adaptive inertia force control. *International Conference on Intelligent Robots and Systems (IROS)*, pages 335 –340, 2003.

K. G. Pearson. Common principles of motor control in vertebrates and invertebrates. *Annual Review of Neurosciences*, pages 265–295, 1993.

F. Plestan, J.W. Grizzle, and E.R. Westervelt. Stable walking of a 7-dof biped robot. *IEEE Transactions on Robotics and Automation*, 19:653–667, 2003.

N. Z. Sasha and E. A. Seyfarth. Exoskeletal sensors for walking. *Annual Review of Neurosciences*, pages 86–90, July 1996.

G. Taga, Y. Yamaguchi, and H. Shimizu. Self-organized control of bipedal locomotion by neural oscillators in unpredicatble environment. *Biological Cybernetics*, 65:147–159, 1991.

A. Takanishi, M. Ishida, Y. Yamazaki, and I. Kato. The realization of dynamic walking by the biped robot. *Proceedings of the International Conference on Advanced Robotics, Tokyo*, WL-10RD:459–466, 1985.

C. L. Vaughan. Theories of bipedal walking: an odyssey. *Journal of Biomechanics*, 36:513–523, 2003.

M. Vukobratovic, B. Borovac, D. Surla, and D. Stokic. *Biped locomotion: dynamics, stability, control and applications*, volume 7 of *Scientific Fundamentals of Robotics*. Springer-Verlag, Berlin, 1989.

E. R. Westervelt, J. W. Grizzle, and D. E. Koditschek. Hybrid zero dynamics of planar biped walkers. *IEEE Transactions on Automatic Control*, 48:42–56, 2003.

B.E. Willer and W.L. Miranker. Neural organization of the locomotive oscillator. *Biological Cybernetics*, 68:307–320, 1993.

D.A. Winter. *Biomechanics and motor control of human movement*. John Wiley & Sons, 2nd edition, 1990.

Appendix A

Locomotion Control with Van der Pol NO

The single NO model as Eq.4.24 shown in Chapter four is utilized to construct a four NOs network. The coupling effect of the NOs result in a fixed phase lag between different NOs. The four NO model can be expressed as below:

$$\ddot{x_1} - \mu_1(\rho_1^2 - x_a^2)\dot{x_1} + g_1^2 x_a = q_1 \tag{A.1}$$

$$\ddot{x_2} - \mu_2(\rho_2^2 - x_b^2)\dot{x_2} + g_2^2 x_a = q_2 \tag{A.2}$$

$$\ddot{x_3} - \mu_3(\rho_3^2 - x_c^2)\dot{x_3} + g_3^2 x_a = q_3 \tag{A.3}$$

$$\ddot{x_4} - \mu_1(\rho_4^2 - x_a^2)\dot{x_1} + g_4^2 x_a = q_4 \tag{A.4}$$

where

$$x_a = x_1 - \lambda_{21} x_2 - \lambda_{31} x_3 \tag{A.5}$$

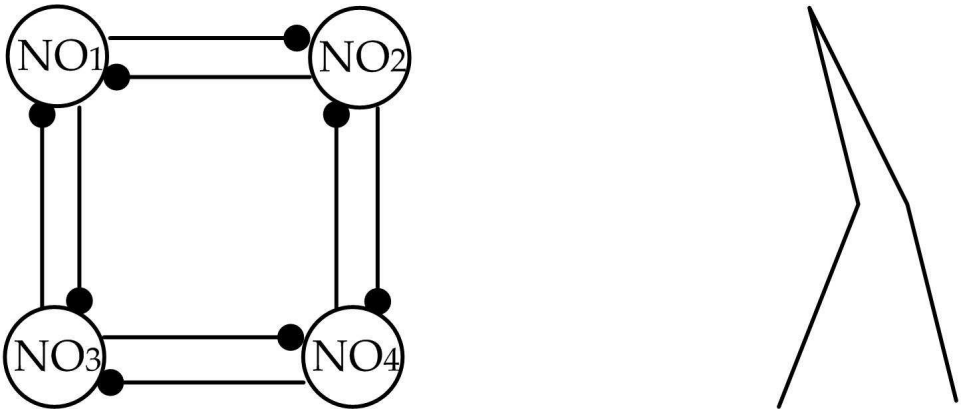

Figure A.1: Network with four coupled Van der Pol NO.

$$x_b = x_2 - \lambda_{21} x_1 - \lambda_{31} x_4 \tag{A.6}$$

$$x_d = x_3 - \lambda_{21} x_1 - \lambda_{31} x_4 \tag{A.7}$$

$$x_d = x_4 - \lambda_{21} x_2 - \lambda_{31} x_3 \tag{A.8}$$

x_1, x_2, x_3 and x_4 and x_a, x_b, x_c and x_d are the inner state of the NO. λ_{ij} is the synaptic weight of inhibitive connection from jth to ith NO.

The CPG network is organized such that one neuron is only inhibited by two neighboring neurons but has no inhibitive connection to the fourth one (***e.g.:*** **NO1** receives inhibition from **NO2** and **NO3** but no inhibition from **NO4**). Table A.1 shows the parameters values of Van der Pol NOs of the CPG.

The output of the NO is mapped directly to the hip and knee angles of (Fig. A.2).

The range of angular variability is set to be $(-50^o, 50^o)$ for hip joint and $(25^o, 45^o)$ for

Table A.1: Parameters of of Van der Pol NOs

Parameters			
$\mu_1 = 1,$	$\mu_2 = 2,$	$\mu_3 = 1,$	$\mu_4 = 2$
$\rho_1 = 2,$	$\rho_2 = 1,$	$\rho_3 = 2,$	$\rho_4 = 1$
$g_1 = 17,$	$g_2 = 20,$	$g_3 = 17,$	$g_4 = 20$
$q_1 = 12,$	$q_2 = -20$	$q_3 = 12,$	$q_4 = -20$
$\lambda_{13} = 0.2,$	$\lambda_{31} = 0.2,$	$\lambda_{12} = -0.2,$	$\lambda_{21} = -0.2$
$\lambda_{24} = 0.2,$	$\lambda_{42} = 0.2,$	$\lambda_{34} = -0.2,$	$\lambda_{43} = -0.2$

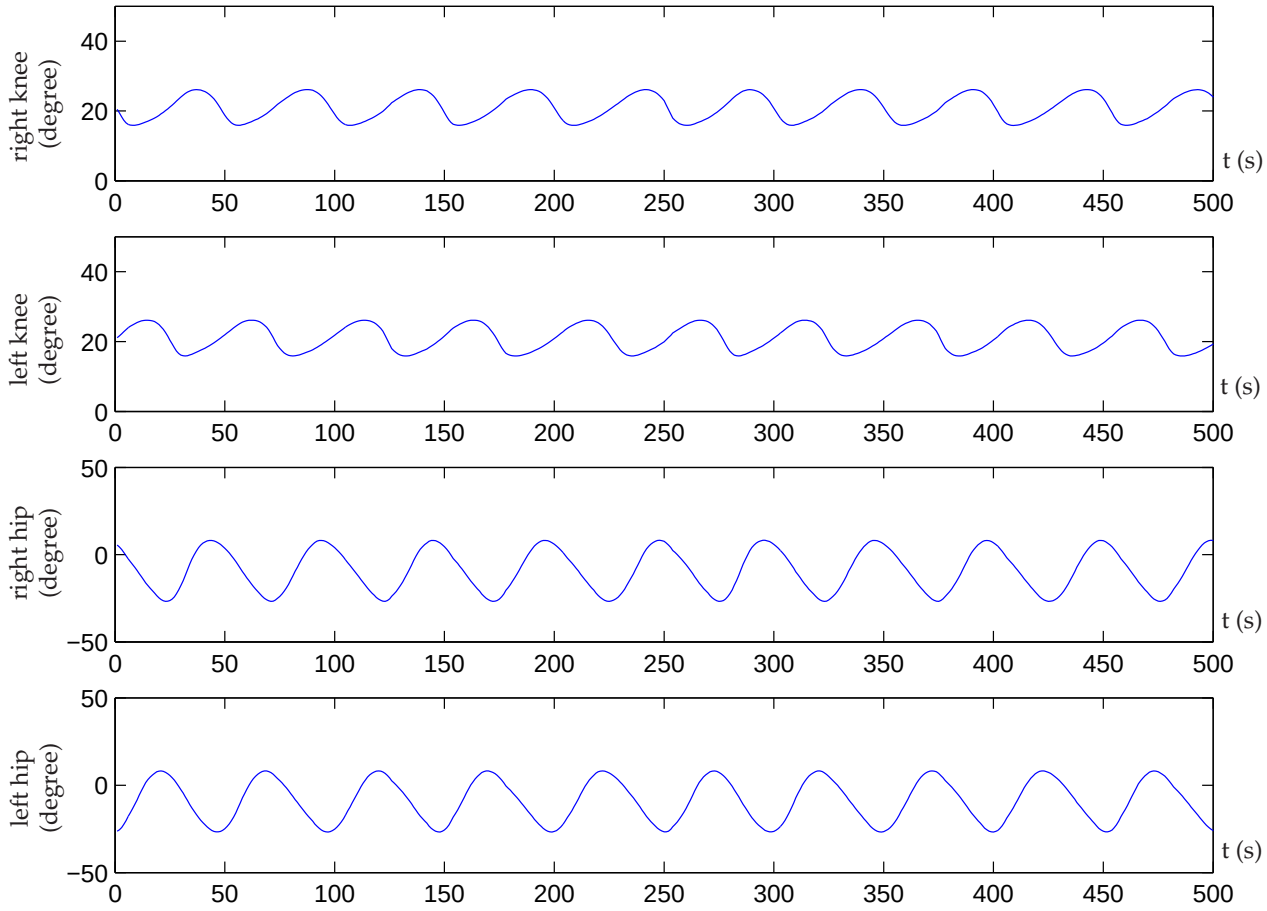

Figure A.2: Neural activities of four Van der Pol Bipedal

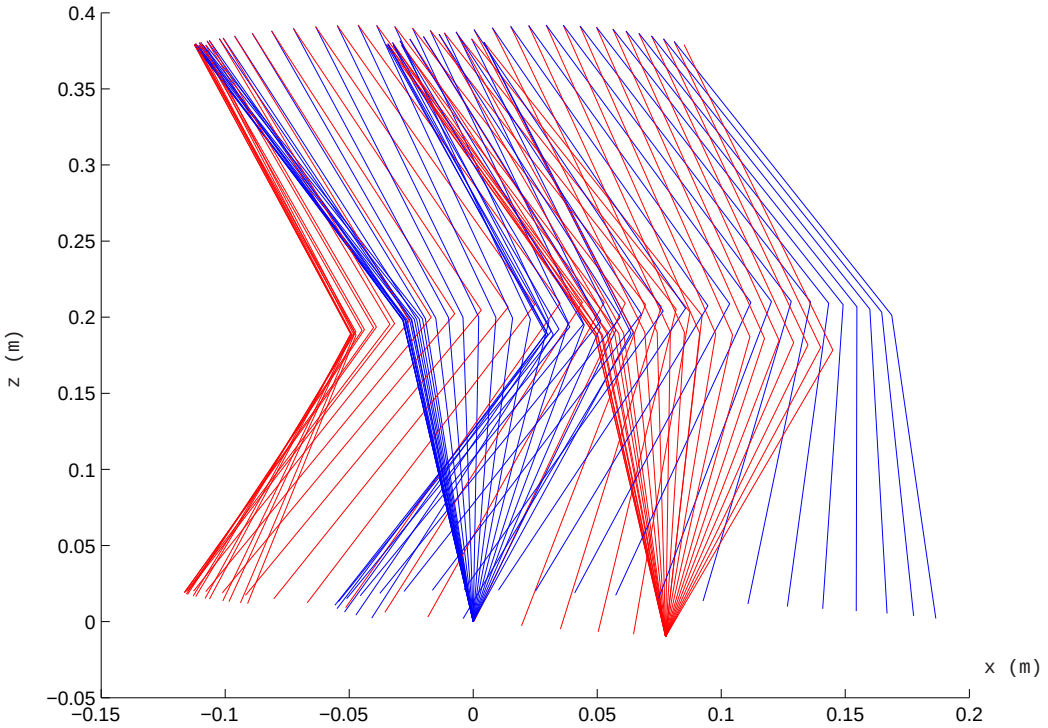

Figure A.3: Stick diagram of bipedal robot

knee joint.

The stick diagram of the bipedal robot in one walking cycle is presented in Fig.A.3. The CPG network shows a decent capability in generating the walking pattern.